

**University of Szeged**  
**Faculty of Pharmacy**  
**Institute of Pharmaceutical Technology and Regulatory Affairs**

Head: Dr. habil. Ildikó Csóka PhD

**Ph.D. thesis**

**RESEARCH AND DEVELOPMENT OF NANOSIZED DRUG CONTAINING NASAL  
DRUG DELIVERY SYSTEMS TO REACH SYSTEMIC AND CENTRAL NERVE  
SYSTEM EFFECT**

**By**

**Péter Gieszinger**

**Pharmacist**

**Supervisor:**

**Dr. Rita Ambrus habil. PhD**

**SZEGED**

**2020**

## **PUBLICATIONS RELATED TO THE SUBJECT OF THE THESIS**

1. Gieszinger P., Bartos Cs., Szabó-Révész P., Ambrus R.- Nazális készítmények aktualitásai; bevételre alkalmas eszközök és modern szerelékek. *GYÓGYSZERÉSZET* 61:(4) pp. 204-211. (2017)
2. Gieszinger P., Csoka I., Pallagi E., Katona G., Jojart-Laczkovich O., Szabó-Révész P., Ambrus R.- Preliminary study of nanonized lamotrigine containing products for nasal powder formulation. *DRUG DESIGN DEVELOPMENT AND THERAPY* 11: pp. 2453-2466. (2017) IF: 3.254 – Q1 journal
3. Gieszinger P., Tomuta I., Casian T., Szabó-Révész P., Ambrus R.- Definition and validation of the Design Space for co-milled nasal powder containing nanosized lamotrigine. *DRUG DEVELOPMENT AND INDUSTRIAL PHARMACY* 44 : 10 pp. 1622-1630. , 9 p. (2018) IF: 2.367 – Q2 Journal
4. Ambrus R., Gieszinger P., Gáspár R., Sztojkov-Ivanov A., Márki Á., Janáky T., Tömösi G., Kecskeméti G., Szabó-Révész P., Bartos Cs.- Investiagtion of the absorption of nanosized lamotrigine containing nasal powder via the nasal cavity. *MOLECULES*, 25: 1065. IF: 3.060 - Q1 Journal (2020); doi:10.3390/molecules25051065.
5. Gieszinger P., Csaba S. N., Garcia-Fuentes M., Prasanna M., Szabó-Révész P., Ambrus R.- Preparation and characterization of lamotrigine containing nanocapsules for nasal administration. *EUROPEAN JOURNAL OF PHARMACEUTICS AND BIOPHARMACEUTICS*. Under review. – Q1 journal
6. Gieszinger P., Katona. G., Szabó-Révész P., Ambrus R.- Stability study of nasal powder formulation containing nanosized lamotrigine. *ACTA PHARMACEUTICA HUNGARICA*. Under review. - Q4 journal

## **PRESENTATIONS RELATED TO THE THESIS**

### **Oral presentations**

1. Gieszinger P.- Nanonizált lamotrigint tartalmazó intranazális gyógyszerforma előállítása és vizsgálata. Tudományos Diákköri Konferencia, Szeged (2016)
2. Gieszinger P.- Ko-örléssel előállított, nanonizált lamotrigint tartalmazó nazális gyógyszerforma vizsgálata. XII. Clauder Ottó emlékversenly, Budapest (2016)
3. Gieszinger P. Nanonizált hatóanyag tartalmú nazális por előállításának optimalizálása. Szegedi Tudományegyetem Sófi József a Szegedi Tehetségekért Alapítvány Ösztöndíj Konferencia, Szeged (2018)
4. Gieszinger P.- Design Space meghatározása és validálása nanonizált lamotrigin tartalmú nazális por előállítása céljából. Richter Gedeon Nyrt. I. Fiatal Technológusok Fóruma, Budapest (2018)
5. Gieszinger. P., Ambrus R., Szabó-Révész P. - Nasal formulation of active ingredients to induce systemic and central nervous system effects. I. Symposium of Young Researchers on Pharmaceutical Technology, Biotechnology and Regulatory Science, Szeged (2019) pp. 22-22., 1 p.
6. Gieszinger P., Csaba S. N., Garcia-Fuentes M., Prasanna M.; Katona G., Szabó-Révész P., Ambrus R. - Lamotrigin tartalmú nanokapszulák fejlesztése. Gyógyszertechnológiai és Ipari Gyógyszerészeti Konferencia: A Magyar Gyógyszerésztudományi Társaság Gyógyszeripari Szervezetének és Gyógyszertechnológiai Szakosztályának Konferenciája. Siófok, (2019) pp. 22-22., 1 p. 2019.
7. Gieszinger. P., Ambrus R., Szabó-Révész P.- Formulation of nasal drug delivery systems to induce systemic and central nervous system effect. II. Symposium of Young Researchers on Pharmaceutical Technology, Biotechnology and Regulatory Science, Szeged (2020), pp. 8-8., 1 p.

### **Poster presentations**

1. Ambrus R.\*, Gieszinger P., Pallagi E., Csóka I., Szabó-Révész P.- Formulation of a nasal powder containing nanonized antiepileptic Lamotrigine, by applying the QbD approach. 11th Central European Symposium on Pharmaceutical Technology 2016, Belgrade, Serbia
2. Gieszinger P.\*, Casian T., Tomuta I., Szabó-Révész P., Ambrus R.- Development of a nasal powder preformulation process by Design of Experiment method. ACTA PHARMACEUTICA HUNGARICA 87:(043) Paper P2B-4. 1 p. 7th BBBB International Conference on Pharmaceutical Sciences. 2017, Balatonfüred, Hungary
3. Ambrus R., Gieszinger P., Szabó-Révész P., Sztójkov-Ivanov A., Ducza E., Márki Á., Gáspár R., Kecskeméti G., Janáky T., Bartos Cs.- *In vitro* and *in vivo* characterization of nasal powder containing nanonized lamotrigine. 12th Central European Symposium on Pharmaceutical Technology and Regulatory Affairs 20-22.09. 2018, Szeged, Hungary
4. Gieszinger P., Csaba S. N., Garcia-Fuentes M., Prasanna M., Szabó-Révész P., Ambrus R.- Preparation and characterization of lamotrigine containing nanocapsules for nasal administration. 3rd European Conference on Pharmaceutics - Bringing science into pharmaceutical practice p. 21. 2019, Bologna, Italy
5. Gieszinger P., Szabó-Révész P., Ambrus R.- Nanonizált lamotrigin tartalmú nazális porok stabilitásvizsgálata. Congressus Pharmaceuticus Hungaricus XVI. 2020, Debrecen, Hungary

## Table of contents

1. INTRODUCTION .....	1
2. AIMS OF THE WORK.....	2
3. LITERATURE BACKGROUND OF THE RESEARCH WORK .....	3
3.1. Biopharmaceutical aspects of nasal drug delivery .....	3
3.1.1. Nasal products on the market .....	4
3.1.2. Nasal powders as potential dosage forms in different therapies.....	6
3.1.3. Formulation aspects of nasal dosage forms.....	6
3.1.4. Nasal form investigations.....	7
3.2. General review and engineering possibilities of nanoparticles .....	8
3.2.1. Powders containing nanosized API .....	9
3.2.2. Nanocapsules as novel therapeutical nanosystems.....	10
3.3. Quality by Design.....	10
4. MATERIALS AND METHODS.....	11
4.1. Materials .....	11
4.2. Methods .....	12
4.2.1. Identification of factors affecting product quality .....	12
4.2.2. Initial RA of nasal powder .....	13
4.2.3. Experimental Design of nasal powders.....	13
4.2.4 Dry milling method for nasal powder production .....	14
4.2.5. Nanocapsule production.....	15
4.2.6. Micrometric investigation methods .....	16
4.2.7. Structural investigations.....	17
4.2.8. <i>In vitro</i> studies .....	17
4.2.8.1. Development of <i>in vitro</i> permeability investigation method.....	18
4.2.9. <i>In vivo</i> studies .....	21
4.2.10. Stability measurements .....	23
5. RESULTS AND DISCUSSION.....	24
5.1. Development of NP formulation .....	24
5.1.1. Knowledge space development and RA .....	24
5.1.2. Investigation of NP formulations .....	25
5.1.2.1. Micrometric properties.....	25
5.1.2.2. Structural investigations.....	26
5.1.2.3. Dissolution and permeability tests of the samples .....	27
5.1.3. Definition and validation of the Design Space of the NP samples .....	28
5.1.4. <i>In vivo</i> studies .....	33
5.1.5. Stability study of the nanoLAM powder.....	34
5.2. Development of NC formulations .....	34
5.2.1. Identification of factors affecting product quality .....	35

5.2.2. Particle size, particle size distribution and surface charge characterization of NCs.....	36
5.2.3. Encapsulation efficacy (EE) and drug loading (DL) .....	37
5.2.4. Particle morphology.....	37
5.2.5. <i>In vitro</i> drug release and permeability studies .....	37
5.2.6. <i>In vivo</i> drug release study.....	38
5.3. Comparison of NP and NC formulations based on their <i>in vivo</i> performance.....	40
6. CONCLUSION.....	41
REFERENCES .....	44
ACKNOWLEDGMENTS .....	2

## ABBREVIATIONS

<b>API</b>	Active pharmaceutical ingredient
<b>AUC</b>	Area under curve
<b>BBB</b>	Blood-brain-barrier
<b>BCS</b>	Biopharmaceutical classification system
<b>CNS</b>	Central Nervous System
<b>CPP</b>	Critical Process Parameter
<b>CQA</b>	Critical Quality Attribute
<b>DoE</b>	Design of experiment
<b>DS</b>	Design space
<b>DSC</b>	Differential scanning calorimetry
<b>DTE</b>	Drug targeting efficiency
<b>EMA</b>	European Medicines Agency
<b>FDA</b>	Food and Drug Administration
<b>FDNCs</b>	Freeze-dried nanocapsules
<b>GI</b>	Gastrointestinal tract
<b>IV</b>	Intravenous
<b>J</b>	Flux
<b>K<sub>p</sub></b>	Permeability coefficient
<b>LAM</b>	Lamotrigine
<b>LC-MS</b>	Liquid chromatography-mass spectroscopy
<b>LEV</b>	Levodopa
<b>MCC</b>	Mucociliary clearance
<b>MEL</b>	Meloxicam
<b>NaHA</b>	Sodium hyaluronate
<b>NCs</b>	Nanocapsules
<b>NP</b>	Nasal powder
<b>PDI</b>	Polydispersity index
<b>PgP</b>	P-glycoprotein
<b>PM</b>	Physical Mixture
<b>PS</b>	Particle size
<b>PVA</b>	Polyvinyl alcohol
<b>PVP</b>	Polyvinyl pyrrolidone
<b>QbD</b>	Quality by Design
<b>QTPP</b>	Quality Target Product Profile
<b>RA</b>	Risk assessment
<b>SEM</b>	Scanning Electron Microscopy
<b>SNES</b>	Simulated nasal electrolyte solution
<b>XRPD</b>	X-ray powder diffraction

# 1. INTRODUCTION

Nasal drug delivery has received remarkable attention in the past few decades, because the nose offers a great alternative administration route due to its special anatomy and physiological properties. Via nasal application, local, systemic and central nervous system effects are also available and despite the fact that the majority of products are for local use (e.g. decongestants), an increasing number of products with systemic and CNS effect is on the market. The fact that nasal formulations are not just for local therapy, makes them attractive in the therapy of CNS diseases (e.g. epilepsy, Parkinson's disease, Alzheimer's disease). Nasal administration is pain-free, whilst rapid onset of action can be achieved; therefore, enhanced patient adherence can be accomplished.

Most of the APIs used nowadays are in BCS II, which means that these drugs have low solubility and high permeability. One of the most popular ways to improve the solubility of APIs is particle size reduction, including nanonization. Nanosized drugs can provide higher bioavailability due to their smaller particle size and larger specific surface. There are different kinds of technologies with which nanosystems can be produced. The two main groups are bottom-up and top-down technologies. In the case of the bottom-up technology, micro or nanoparticles are built up from dissolved drug molecules, while in the case of the top-down approach, the raw material is subsequently broken down. Both approaches were applied in this project as NP formulations were produced with a top-down (co-milling) method, while NCs were produced with a bottom-up (solvent displacement) technique.

QbD is a holistic and systematic quality management method, where the development design is risk and knowledge-based. The foundation of a QbD-guided development is RA which can be initial, updated, or final. Good RA results are essential for designing the researches more efficiently and economically in practice, which makes the studies ecologically friendly, time and cost-effective. The thesis reports the development and investigation of two nasal formulations that contain nanosized lamotrigine in order to use them in the therapy of epilepsy as alternative dosage forms of the traditionally applied tablets.

Time and cost-effectiveness are key elements during the pharmaceutical research and development of different formulations. Thus, the development of proper *in vitro* models is exceedingly significant from an economical and ecological aspect. In the case of nasal formulations, due to the unique anatomical and physiological properties, many aspects need to be considered during the development procedure. One of the most important factors is the permeability rate of the product across the membrane, so its accurate detection is particularly important during the development.

## 2. AIMS OF THE WORK

The aim of this PhD work was to research, develop and investigate LAM-containing nasal formulations to induce systemic and CNS effect (Figure 1.). Accordingly, the goal was to develop nanosized LAM-containing nasal dosage forms, which could be great alternatives to marketed tablets in the therapy of epilepsy. The parts of the project were the following:

- I. Literature review of nasal drug delivery, nanosystems, and QbD methodology in order to lay the theoretical foundations of the development of QbD-based, nanosized LAM-containing nasal formulations, which would be produced with a top-down and a bottom-up method. The reason this field was chosen that despite the well-known advantages of the nasally used formulations, just a few nasal powders or nasally administered NCs can be found on the market.
- II. QbD based RA for NP delivery, identification, prioritization, and selection of the most influencing CQAs, CPPs of NP production with the tools of QbD. Preliminary study of the nanosized API containing NP and selection of the most promising additive. Optimization of the dry milling process with DoE, which meant the Design Space determination and validation of the powder production.
- III. Micrometric and structural investigation of NP formulation, moreover the implementation of *in vitro* and *in vivo* investigations, and parallelly the development, adaptation and validation of a novel *in vitro* horizontal permeability method.
- IV. QbD based RA for LAM encapsulation, which consisted of the identification, prioritization, and selection of the most influencing factors using an Ishikawa diagram. Development, optimization, and production of LAM containing NCs, which meant the determination of formulation components, their ratios and the process parameters.
- V. Micrometric and structural investigations of NP formulation, and the implementation of *in vitro* and *in vivo* investigations.
- VI. Comparison of NC and NP samples, and based on the *in vivo* performance of formulations and finally, make a suggestion which formulation could be used as an innovative delivery system in the therapy of epilepsy.

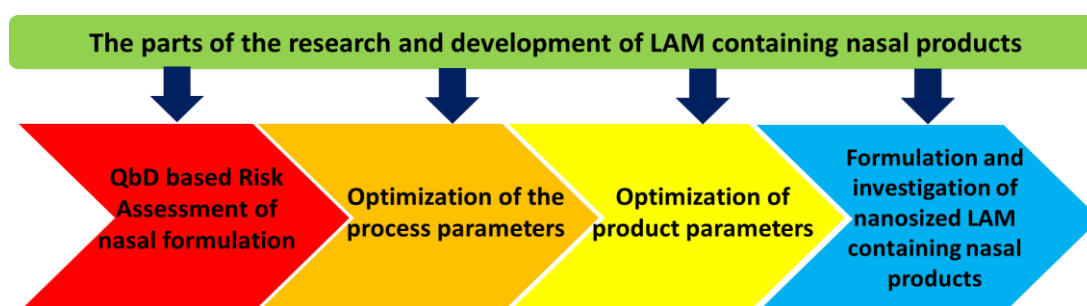


**Figure 1.** The aims of the PhD work



### **3. LITERATURE BACKGROUND OF THE RESEARCH WORK**

#### **3.1. Biopharmaceutical aspects of nasal drug delivery**

The nasal cavity – as an alternative route of drug administration – became very important in the past years. Due to its unique anatomical and physiological properties, the nose can be a major, alternative drug administration route and nasal formulations can offer a major breakthrough in different therapies [1,2]. The nasal cavity can be divided into two main regions: the olfactory and the respiratory region. The mucosa of the respiratory region, which takes up ~ 90% of the surface, is responsible for respiration, the regulation of humidity and temperature of inhaled air, as well. The remaining ~10 % of the area is the olfactory region which is responsible for olfaction. It is located high in the nasal cavity. It overlies the cribriform plate that has a bony structure with many pores. These pores allow the neuronal bundles from the olfactory region to pass into the CNS. However, it is important to note that besides the olfactory nerve, CNS effect can be achieved via the trigeminal nerve [3]. It is possible because the neurons from the branches of the trigeminal nerve pass directly through the mucosa (Figure 2.) [4–7].

If taken nasally, APIs can reach their site of action in several ways. Once on the respiratory mucosa, they can get directly into the systematic circulation – or if the particle size is inappropriate the API can reach the lungs and then the systemic circulation –, which results in increased plasma concentration in a short time. This is the so-called nose to blood delivery. However, the API cannot stay on the mucus for longer than 15-20 minutes due to the unique physiological process of the nose. The so-called MCC renews the nasal mucosa continuously, which means that after some time the API gets into the GI tract through the nasopharynx. From this part, the API can also be absorbed into the systemic circulation. Once in the bloodstream, the drug can reach any part of the body, including the brain tissues. To do this, however, it has to pass through the BBB which is the major limiting factor if the aim is to reach CNS effect, but these will be detailed later [8–10]. Yellow arrows mark this possible route in Figure 2.

Marked with red arrows in Figure 2. is another possibility. In this case, the API reaches the CNS directly through the trigeminal and the olfactory nerves. This can occur because of the free nerve endings (mentioned above) and the so called axonal transport which increases the drug concentration in the brain tissues [11]. This kind of nose-to-brain delivery can be advantageous e.g. in neurological diseases, pain management or brain tumors [12–16].

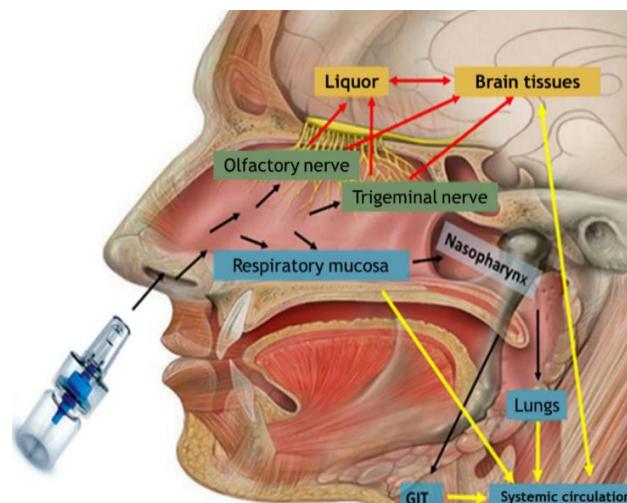


**Figure 2.** The possible routes of API in case of nasal administration.

If drugs are taken nasally, there are many advantages and opportunities due to the unique properties of the nose. First of all, local, systemic and CNS effects are available. It can be useful if the API undergoes extensive hepato-gastrointestinal metabolism in the GI tract or the drug is irritative or decompose in the GI tract. On the other hand, if there is no or limited metabolism, lower doses are sufficient to reach the therapeutic level, thus, GI and other side effects become reduced [7]. Another advantage is that the drug administration is painless, and sterility is not required. Moreover, the nasal mucosa is highly vascularized and has a large surface, which means that the surface of an average human nasal mucosa is approximately 200 cm<sup>2</sup>. These properties provide a great opportunity for high permeability and rapid drug absorption that leads to a rapid onset of action [17–19].

In spite of the high potential, nasal drug delivery has some obvious drawbacks. Nasal formulations cannot be used for a longer period as they may damage the nasal mucosa. The above mentioned MCC limits the residence time on the mucosa and the BBB limits the access to the CNS as particles over ~300 Da are not able to get into the brain tissues. Lipophilicity and surface charge are also critical because hydrophilic and charged particles cannot pass the BBB. Further limiting factors are nasal enzymatic degradation, limited nasal volume, Pgp efflux transporters, pathological changes (e.g. runny nose, polyps). These can worsen the efficiency of nasal administration [4,20].

### 3.1.1. Nasal products on the market

Although it has been discovered for centuries that nasal formulations can be used in some illnesses, their main application was limited to local diseases until the past one or two decades. Accordingly, most of the marketed products are solution-based drops or sprays. The reason is that these formulations are safe, easy-to-use and cheap, the dosage is uniform and they have been used for decades, so people have got used to them [21]. On the Hungarian market, there are 124 marketed nasal products (8 medical products, 116 medications)

including 113 liquid sprays or drops, 6 ointments, and just 1 powder formulation. This means that 94.4 % of the formulations are drops or sprays (Figure 3.).

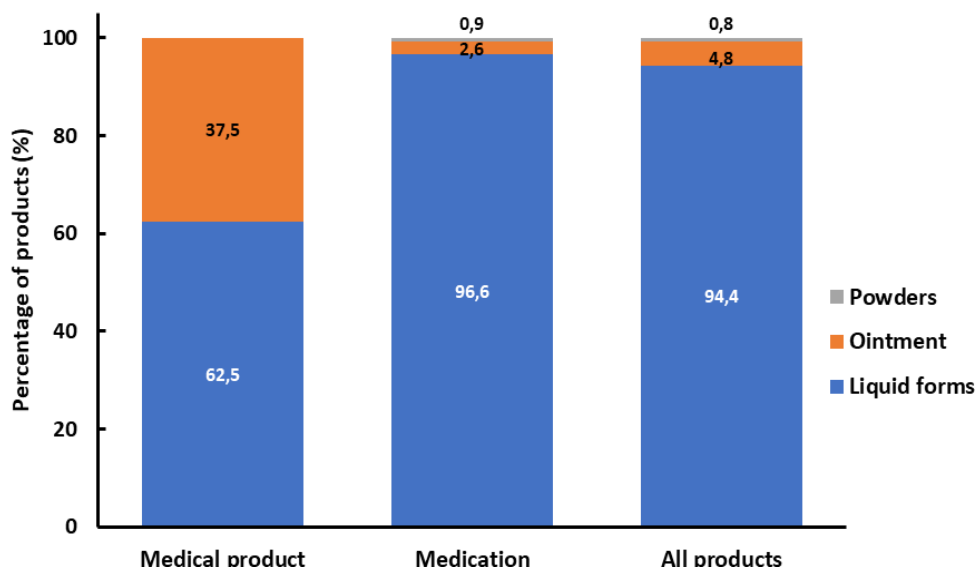


**Figure 3.** The distribution of nasal products on the Hungarian market [22]

Though the most marketed products have localized effect and used mainly in rhinitis or allergic diseases, this tendency has changed a bit as the application of nasal formulations has extended. Besides the well-known products, there are formulations for the treatment of pain management, diabetes insipidus, migraine, hormone-dependent prostate carcinoma, postmenopausal osteoporosis, etc. Moreover, there are researches for the formulation of nasal products for Alzheimer’s disease, Parkinson’s disease, epilepsy and many other therapies [8,19,23].

Epilepsy is a common, neurological disease, which is characterized by recurrent, unexpected seizures. These seizures are caused by excessive, synchronous or neuronal activity in the brain. One of the biggest challenges is that in spite of the epilepsy treatment approximately 20–30% of patients experience break-through seizures. In these cases, oral or intravenous intervention is really difficult and dangerous, alternative routes of administrations are required. There are existing rectal formulations of benzodiazepines, but this administration route is understandingly unpopular, so there is a need for both acute and chronic treatment using multiple types of formulations [24, 25].

Intranasal administration of antiepileptic drugs is a promising possibility due to the previously mentioned advantages from which rapid onset of action stands out [26]. Accordingly, there have been some efforts for the formulation of lamotrigine or midazolam [27]. Midazolam has been extensively investigated in epilepsy and some guidelines recommend it as an alternative drug delivery for prompt treatment [28].

In the past few years, nasal powders have gained considerable attention due to the many advantages they possess. On the market, there is a poor number of nasal powders used in the therapy of migraine and allergic or vasomotor rhinitis [29,30], but in the next few years, the

number of formulations will probably increase. Moreover, the FDA has recently approved a new product for the treatment of severe hypoglycemia [31].

### **3.1.2. Nasal powders as potential dosage forms in different therapies**

Dry powder formulations are becoming widespread nowadays (oral powders, dry powder inhalations, nasal powders) [32–34]. One of the main reasons for the increasing number of formulations is that fewer adjuvants are needed during the formulation process. Thus, they offer better physicochemical and microbiological stability than liquid formulations. As a result, preservatives are not required and also unexpected incompatibilities rarely occur in powder formulations. Their shelf life is longer and transport is much easier, but packaging must ensure protection against humidity and light [17, 35].

Nasal powders (NPs) are formulated to have favorable physicochemical and microbiological qualities and stability. Also, the administration dose can be higher compared to liquid formulations as the nasal mucosa can accommodate 15-25 mg of powder per nostril per shot, while only a maximum of 200  $\mu$ l per spray in liquid formulations [36]. Nasal powder have high adhesion ability and, therefore, the residence time can be prolonged, which provides better absorption through the nasal mucosa, thus, higher bioavailability [37]. Moreover, the administration of appropriate adjuvants can slow MCC [38]. As we have discussed before, with nasal powders, rapid onset of action can be reached that can be extremely advantageous in cases, when rapid intervention is essential (e.g. migraine, pain management) [39].

The quality recommendations and quality requirements concerning NPs are included in international regulations and guidelines discussing the nasal and inhalational products. From a regulatory point of view, nasal products as powerful drug delivery systems are special because their design, development, and optimization should be parallel with those of the delivery device (e.g., NP inhaler, NP sprayer, NP insufflators) to assure proper dosing. For dry powders, the related European Medicines Agency (EMA) and US Food and Drug Administration (FDA) guidelines recommend special attention to and critical thinking about the following: 1) drug substance specifications, such as particle size (in related literature, it is recommended to be around 40  $\mu$ m), particle size distribution, crystalline form, shape and crystallinity which could be critical for product and aerodynamic performance; 2) excipient specifications and 3) testing of humidity and temperature sensitivity [40–43].

### **3.1.3. Formulation aspects of nasal dosage forms**

In order to achieve a systemic or CNS effect, intranasal formulations usually contain different additives to ensure the appropriate viscosity [44], pH (in compliance with the pH of the nasal cavity), better mucoadhesion, longer residence time [45], higher permeability rate and often [46], controlled release of the API. Due to the MCC in the nasal cavity, the formulation of

viscous and mucoadhesive products is needed to reach prolonged contact time with the nasal mucosa, thus, enhancing the delivery of the drugs [47] and making therapies more efficient. The range and use of applied excipients are wide. To increase the viscosity (cellulose derivatives) and the mucoadhesive strength (carbomers, chitosans, lectins, thiomers, alginate poly(ethylene glycol acrylate) or Poloxamer) of the intranasal formulation, many additives can be used [48,49]. Sodium hyaluronate (HA) is one of the most important and most commonly used mucoadhesive and biocompatible agent. This anionic, natural polysaccharide owns great mucoadhesive capacity [50], low immunogenicity and high biocompatibility [51]. Moreover, it can improve the absorption of drugs and proteins via mucosal tissues [52]. However, to ensure controlled drug delivery, other polymers (PVA, PVP,  $\alpha$ -cyclodextrins) are also applied [53].

The solubility of the API, the size and mass of the molecule, the  $pK_a$  value, the polarity, the rate of dissolution and permeability need to be highly considered when formulating nasal products [54]. All of the mentioned properties can be improved by size reduction to the micro or nano range and, thus, micronization and nanonization could be a great choice in order to prepare formulations for poorly water-soluble drugs with increased bioavailability [55, 56].

#### **3.1.4. Nasal form investigations**

In addition to the usual investigations, nasal formulations are needed to be tested specifically. According to the Pharmacopeia, many properties of the nasal formulations should be investigated such as uniformity of mass, API content or particle size. It is also desirable to perform other tests specific to the particular formulation [57, 58].

In the case of the product, permeability is one of the most influencing factors of quality. Therefore, an accurate, easy, well-reproducible and robust technique is extremely important during the development of a nasal product [59]. There are many ways to measure permeability and these are available on the market, but in our opinion, a more complex method could be developed. Most of the devices used are vertical, such as the commonly used Franz cell, but there are some devices with a horizontal layout. In all devices, there is a donor and an acceptor phase, which is separated by a semipermeable membrane in order to model the physiological conditions of the human body [60]. It is advantageous if the diffusion cells can be tempered and continuous magnetic stirring is possible. Moreover, it is also desirable to use an inline technology, which means that the measurement can be screened in real-time. It is useful because in case of an adverse event (e.g. membrane rupture), the investigation can be interrupted, so it is not detected at the end of the investigation. This makes this approach time and cost effective over offline techniques. Other advantages of inline measurements include easy implementation, reproducibility, independence from the implementor, and no need for constant supervision.

As the device plays a quite important role in the efficacy of nasal administration, its selection and investigation are essential during the development process. Device type depends on the dosage form, the number of doses, the indication of the API and many other parameters. The key factors, which are always investigated, are robustness, dose uniformity and packaging integrity, but several other properties are also investigated before approval [61].

### 3.2. General review and engineering possibilities of nanoparticles

Nanonization is an up-to-date research topic in almost every scientific field. In the pharmaceutical sector, particle size reduction to the micro or nano range is a promising way to improve the dissolution rate of poorly water-soluble drugs [62–64]. The size of nanoparticles is in the range of 1-1000 nm [65]. Nanonization can provide decreased particle size, and parallelly, increased specific surface area, which leads to an increased contact surface for API particles (Figure 4.) [66–69]. Thus, nanonization can result in improved drug dissolution rate [70] and pharmacokinetics [71], while the appearance and intensity of systemic side effects might also decrease [72,73]. All in all, nanonization, in some cases, can lead to improved bioavailability, which is still highly desirable, which can result in a breakthrough in drug administration via alternative routes [74]. The possible, but not sufficiently proven drawback of nanonization is the so-called nanotoxicity, which is the harmful accumulation of nanoparticles in tissues and organs [75].

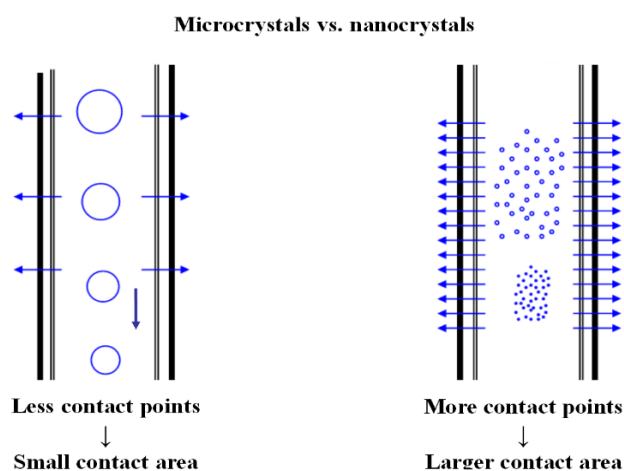


**Figure 4.** Due to the smaller particle size and larger specific surface, nanoparticles have higher contact surface with membranes [76]

Several methods exist for the preparation of nanoparticles, which can be divided into two main groups: top-down and bottom-up processes [76]. Top-down methods (such as co-grinding with additives) produce micro or nanoparticles by using mechanical stress. These technologies are environmentally and economically advantageous because they are organic solvent-free, simple and well reproducible. In this case, nanoparticles are produced by grinding the drug together with additives which are responsible for the stability and maintenance of the uniqueness of the particles [77, 78]. Nanoparticles are controlled by adhesive forces and, if the particles are not stabilized, they may coagulate because of the high

particle mobility. Different additives are used to stabilize these particles: polysorbate, hydroxypropyl methylcellulose, Poloxamer, PVP, etc. [79]. PVA is frequently used as a stabilizer, coating the particles and promoting their separation from each other.

Bottom-up technologies (e.g. nanoprecipitation, API encapsulation) are also used for producing nanoparticles. These techniques involve a poorly water-soluble drug, a suitable solvent, and a miscible anti-solvent. The process is based on the principle of transferring the API from the molecular state to a precipitated state under continuous stirring, which leads to the growth of nanoparticles. The solvents are needed to be completely miscible and suitable for the formation of nanosuspensions, drug nanocrystals, or nanodispersions. The advantages of these methods are that they are robust and well-reproducible. Possible disadvantages are the presence of possibly toxic organic solvents, the separation of nanoparticles takes time and experienced implementors are needed to execute the preparation method, while just really low drug concentration is available [76].

In the last decade, the encapsulation of APIs, which is a kind of bottom-up process, has become increasingly important due to its advantages over traditional technological methods for solubilization (e.g. solid dispersions, amorphization). The additives which can be used during the formulation are diverse, but liquid oils and surfactants are the most commonly used adjuvants. The core-shell nanosystems can also be covered with many polymers in order to protect the oily, liquid core. One of the most commonly used polymer is chitosan, which can increase the adhesion property of NCs and extend their residence time on the mucosal surface [80, 81].

### **3.2.1. Powders containing nanosized API**

As it has been previously discussed, nanosized API-containing powders for nasal drug administration have many advantages that can be combined. With nanoparticles, a smaller dose could be enough to reach the therapeutic level, and the increased specific particle surface can be exploitable on the large nasal mucosal surface. Moreover, if it is desirable, higher doses can be administered via powder formulations, and they can offer longer residence time and better adhesion than liquid formulations. Also, the small particles can enter the systematic circulation or CNS rapidly – it is called a prompt effect in case of nanoparticles – so the rapid onset of action can be even faster with nanoparticles.

However, nanosized APIs cannot be administered on their own. Powder products need to fall into the particle size range 10–45  $\mu\text{m}$ . Below this size, the powder can be inhaled into the lungs, while over this size, the powder cannot reach the nasal mucosa. This means that a proper carrier is needed during the formulation that ensures particle size, good flow properties, and prevents the aggregation of nanoparticles during the storage. This last criterion

is extremely important because aggregation can influence the efficiency of the formulation in the wrong way [80, 81].

### **3.2.2. Nanocapsules as novel therapeutical nanosystems**

Some nanocarriers can improve the solubility of hydrophobic drugs and thereby enhance their bioavailability [84, 85]. NCs, which consist of an oily core and a biodegradable polymer shell, can be produced with bottom-up technologies [86]. This structure can protect the APIs from the physiological environment (e.g. pH and enzymatic degradation) and enhance their permeability through biological barriers [87–89]. Further advantages are that the NCs can reduce drug toxicity and increase their stability; they can facilitate the API transport across mucosal surfaces; and they can provide controlled release. Solid and liquid state NCs have been developed for different administration routes. Among these routes, the oral and the parenteral routes are the most researched, but there have been some efforts to prepare dermal, ocular, or nasal formulations [90,91].

### **3.3. Quality by Design**

QbD is a holistic and systematic quality management method, where the development design is risk and knowledge-based; thus, the experiments in practice can be planned more efficiently even in the development of nasal formulations [92]. In a QbD-based development, the first step is the prior definition of the QTPP (essential parameters from the point of view of the patient and the clinical setting). The next step is the selection of the parameters that influence the QTPP critically. These are the CQAs related to the materials and products, and the CPPs related to the selected production method. The key element of a QbD-guided development is RA, which can be initial, updated or final. Good RA results are essential for designing the studies in practice. RA-based development and screening could be more effective and can be used successfully even in the early development of pharmaceutical products [93–97].

With QbD, the experiments can be planned more economically and efficiently. DoE, a tool of the QbD paradigm, is a systematic approach [98]. It allows the finding of optimal product and/or process parameters and usually provides a larger amount of information from fewer experimental runs. It is available by varying the factors and simultaneously evaluating the effect of multiple variables. DoE is also useful for identifying the individual and interacting factors [99]. Using the response surface, the methodology may lead to the development of DS, which assures the quality of the desired product and can be defined for both the formulation and the process parameters [100].



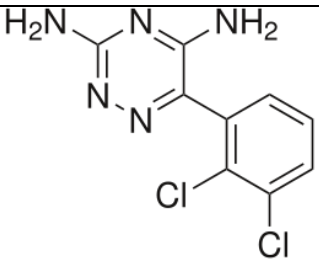
## 4. MATERIALS AND METHODS

### 4.1. Materials

LAM, poorly water-soluble (0.17 mg/mL at 25 °C) second-generation antiepileptic drug of the phenyltriazine class [101,102] was purchased from Teva Ltd. (Budapest, Hungary). The milling additives, polyvinyl pyrrolidone (PVP) ( $M_w=24000$ ) and polyvinyl alcohol (PVA) ( $M_w=27,000$ ), water-soluble synthetic polymer were supplied by ISP Customer Service GmbH (Cologne, Germany). Sodium hyaluronate (NaHA) polymer was purchased from Gedeon Richter Ltd. (Budapest, Hungary).

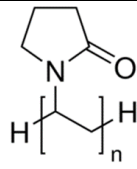
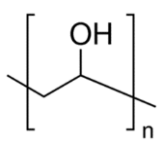
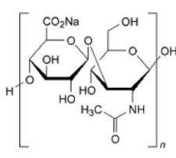
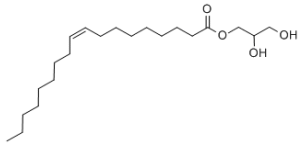
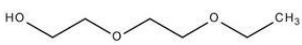
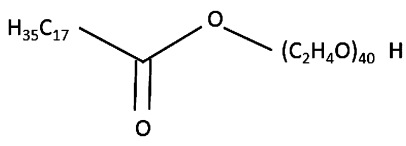
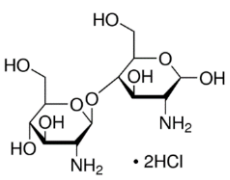
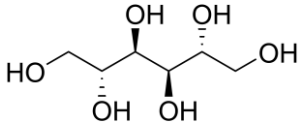
The NC additives: glyceryl monooleate (Type 40) (Peceol<sup>®</sup>) and diethylene glycol monoethyl ether (Transcutol HP<sup>®</sup>) were a kind gift from Gattefossé (St. Preist, France). Polyoxyethylene (40) monostearate (PEG-stearate 40) was purchased from Croda (East Yorkshire, United Kingdom). Chitosan hydrochloride salt was obtained from HMC+ (Halle, Germany). Mannitol was obtained from Sigma-Aldrich (New York, USA). Table 1. and Table 2. show the properties of the applied materials.

**Table 1.** Features of the active agent

	LAM
<b>Chemical structure</b>	
<b>Chemical name</b>	3,5-diamino-6-(2,3-dichlorophenyl)-1,2,4-triazine
<b>Physical properties</b>	white powder, poor water-solubility
<b>Mechanism of action</b>	inhibiting voltage-sensitive sodium channels thereby stabilizing neuronal membranes and consequently modulating presynaptic transmitter release of excitatory amino acids such as glutamate and aspartate
<b>Applications</b>	epilepsy (partial seizures, primary and secondary tonic-clonic seizures, and seizures associated with Lennox-Gastaut syndrome), bipolar disorder (manic period)

The APIs used during the development of *in vitro* permeability method was levodopa (LEV) (L-3,4-dihydroxyphenylalanine) which was obtained from Hungaropharma Ltd.(Hungary) and meloxicam (MEL) (4-hydroxy-2-methyl-N-(5-methyl-2-thiazolyl)-2H-benzothiazine-3-carboxamide-1,1-dioxide) which was obtained from EGIS Ltd. (Budapest, Hungary).

**Table 2.** Properties of additives

	Chemical structure	Physical properties	Application
<b>PVP</b>		white powder	carrier
<b>PVA</b>		yellow or white powder or crystals	carrier, adhesion enhancer
<b>NaHA</b>		white powder	mucoadhesive agent
<b>Glyceryl monooleate (Type 40) (Peceol®)</b>		easily flowing liquid	liquid oil
<b>Diethylene glycol monoethyl ether (Transcutol HP®)</b>		easily flowing liquid	surfactant
<b>Polyoxyethylene (40) monostearate (PEG-stearate 40)</b>		colorless or whitish solid material	surface modifier
<b>Chitosan hydrochloride</b>		white powder	shell component
<b>Mannitol</b>		white powder	cryoprotectant

## 4.2. Methods

### 4.2.1. Identification of factors affecting product quality

As part of the QbD methodology, an Ishikawa diagram was set up to identify a knowledge space of the nasal powder and NC formulations. With the Ishikawa diagram, the identification and systematization of influencing factors were carried out. The factors with the highest influence were chosen and varied.

#### **4.2.2. Initial RA of nasal powder**

To perform the QbD-based initial RA, the first step was the determination of the QTPP of the aimed product. After that, the CQAs and the CPPs of the selected production method were identified. To this identification, a knowledge space development was executed as part of the QbD methodology and an Ishikawa diagram was set up. For performing the RA, the LeanQbD<sup>®</sup> software (QbD Works LLC, Fremont, CA, USA) was used as a technical tool. The first step of RA was to carry out an interdependence rating among the QTPP and CQAs and also among the CQAs and CPPs. A three-level scale was used to describe the relationship between the parameters. Accordingly, the interaction between the elements was described as “high” (H), “medium” (M) or “low” (L). The dynamism of this interdependence rating is presented in tables generated by the software. This was followed by the probability rating step, in which CPPs were estimated and categorized on a 10-point scale. Finally, Pareto charts were generated by the software, presenting the numeric data and the ranking of the CQAs and CPPs.

#### **4.2.3. Experimental Design of nasal powders**

To determine the optimal process parameters a full factorial design was set up with 3 factors on 3 levels, using MODDE 11.1 software (Umetrics, Sweden). The software generated 27 experimental runs as well as 3 center points used to calculate the degrees of freedom, the reproducibility. The milling time (X1), milling speed (X2) and the PVA:LAM ratio (X3) were selected as input variables indicated by RA. To characterize the powders, the following responses were chosen according to RA: average particle size (Y1) and its standard deviation (Y2), the percentage of dissolved LAM from the samples after 5 (Y3) and 10 minutes (Y4). The Factor variation levels and the acceptable ranges of CQAs were chosen based on the RA, prior knowledge and relevant literature. The data fitting and the determination of the statistical parameters were done using the same DoE software. The effects of the independent variables were modeled using the Partial Least Squares method. ANOVA test was applied to evaluate the significance of models ( $p < 0.05$ ). Individual response parameters were evaluated using F-test.

For regression analysis, the goodness of fit, the capacity of prediction, model validity, and reproducibility were considered. The goodness of fit of a model is given by the value of  $R^2$  and represents the variation of the response explained by the model.  $Q^2$  represents the goodness of prediction and reveals how well the model can predict new experiments [100].

Response contour plots were generated to allow illustrate the relationship between the different experimental variables and the responses. Finally, based on experimental results, the DS was determined.

#### 4.2.4 Dry milling method for nasal powder production

PVP, PVA, and NaHA were used for sample preparation as additives to maintain the stability and individuality of nanosized LAM particles. Figure 5. shows the process of sample preparation, where given amount of LAM and additives (1:1, 1:2 and 2:1 ratios) were placed in a Turbula mixer (Turbula System Schatz; Willy A. Bachofen AG Maschinenfabrik, Basel, Switzerland) using 60 rpm for 10 minutes; thus, interactive PMs were prepared.

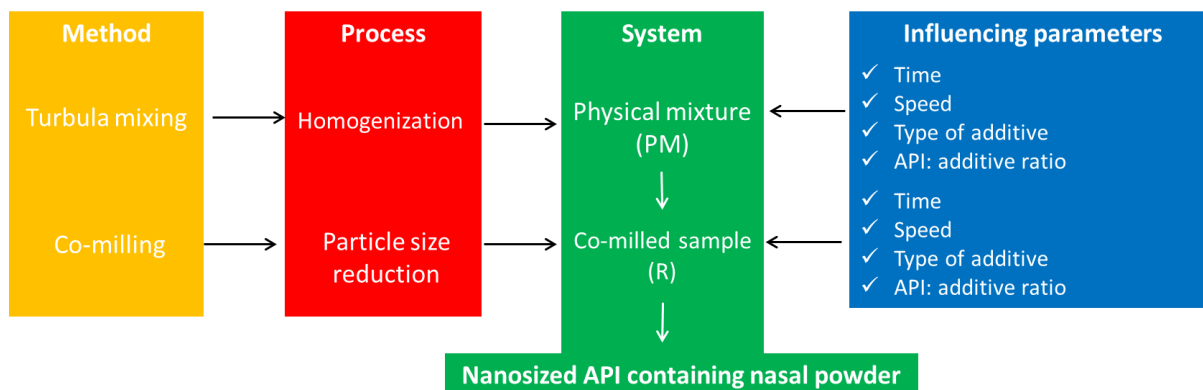


**Figure 5.** The sample preparation protocol of milled samples and PMs [82]

During the preliminary experiments, the effects of three API:additive ratios (1:1, 1:2 and 2:1), milling time (2, 4 and 6 hours) and speed (200, 400 and 600 rpm) were investigated. The optimal parameters of dry milling were selected on the basis of these experiments and can be found in Table 3. The samples are marked with „R”.

**Table 3.** Applied ratios (w/w) and milling parameters for nasal powder formulation

	Ratio	Milling time (h)	Milling speed (rpm)
R_LAM_PVP	1:1	2	400
R_LAM-PVA			
R_LAM-NaHA			

After mixing, the PM samples were placed into a planetary ball mill (Retsch PM 100; Retsch, Neuhausen, Germany), where they were milled for 2 hours at 400 rpm in a 50 mL capacity milling chamber. For milling, 10 steel balls (diameter 10 mm, the weight of each ball 4.02 g) were used to get the co-milled samples. As a comparison, PM samples were used. In those cases, the additives were milled using the same parameters, while after they were mixed with LAM in the above mentioned Turbula mixer using 60 rpm for 10 minutes.

In the case of the DS validated sample, which is called nanoLAMpowder, PVA was used as an additive during the sample preparation process to maintain the stability and non-aggregated property form of LAM particles. NanoLAMpowder was produced as follows: 0.8 g PVA and 1 g LAM were mixed in a Turbula mixer (Turbula System Schatz; Willy A. Bachofen AG Maschinenfabrik, Basel, Switzerland) using 60 rpm for 10 min. After mixing, the sample was placed into a planetary ball mill (Retsch PM 100; Retsch, Neuhausen, Germany) and milled in a 50 mL capacity milling chamber for 1.5 h on 400 rpm with 10 steel balls (diameter 10 mm, the weight of each ball 4.02 g). In the case of PM, PVA was milled for 1.5 h on 400 rpm and

then – according to our previous experiments – it was mixed with non-milled LAM using the same Turbula mixer for 10 mins on 60 rpm.

#### 4.2.5. Nanocapsule production

##### *Solvent displacement method for nanocapsule production*

The NCs were prepared by a solvent displacement method, whose composition (Table 4.) was determined after preliminary experiments. The organic phase was first prepared by adding 100  $\mu$ L of LAM solution (100 mg/mL DMSO solution), 41.7-41.7  $\mu$ L Peceol<sup>®</sup> and Transcutol<sup>®</sup> to 816.6  $\mu$ L PEG-stearate 40 solution (5.33 mg/mL ethanol solution). Then, this solution was poured over 2 mL of ultrapure water upon continuous magnetic stirring. After 10 minutes, 2 mL of chitosan solution (1 mg/mL) was added upon magnetic stirring, leading to the spontaneous formation of the NCs.

**Table 4.** The composition of the NC formulation

<b>LAM solution(100 mg/mL) (<math>\mu</math>L)</b>	100		
<b>Peceol<sup>®</sup> (<math>\mu</math>L)</b>	41.7	+ 2 mL MilliQ water	+ 2 mL 1 mg/mL Chitosan solution after 10 mins
<b>Transcutol<sup>®</sup> (<math>\mu</math>L)</b>	41.7		
<b>PEG-stearate 40 solution (5.33 mg/mL EtOH solution)</b>	ad 1 mL		

After 10 additional minutes of stirring, the NCs were isolated and concentrated to a final theoretical chitosan concentration of 1 mg/mL by centrifugation (Hettich Universal 32 R; Tuttlingen, Germany) at 33000xg for 33 min at 15 °C. In parallel, control blank NCs, without LAM were prepared using the same method.

##### *Freeze-drying method for solid-phase nanocapsule production*

The freeze-drying was performed in Scanvac CoolSafe 100-9 Pro type equipment (LaboGene ApS, Lyngø, Denmark) equipped with a 3-shelf sample holder unit, recessed into the drying chamber. The prepared NCs were lyophilized with 5% mannitol. The process was controlled by a computer program (Scanlaf CTS16a02), the temperature and pressure values were recorded continuously. In the first period of the freeze-drying, the chamber was cooled from room temperature to -25 °C. At this time the vacuum was turned on (p=0,013 mBar). Then the samples were kept under these conditions for 12 hours, while after during the secondary drying the temperature was raised up to +25 °C. temperature. The secondary drying lasted for 4 hours. Thereafter, the freeze-dried NCs (FDNCs) came up. Figure 6. illustrates the process of the NC preparation.

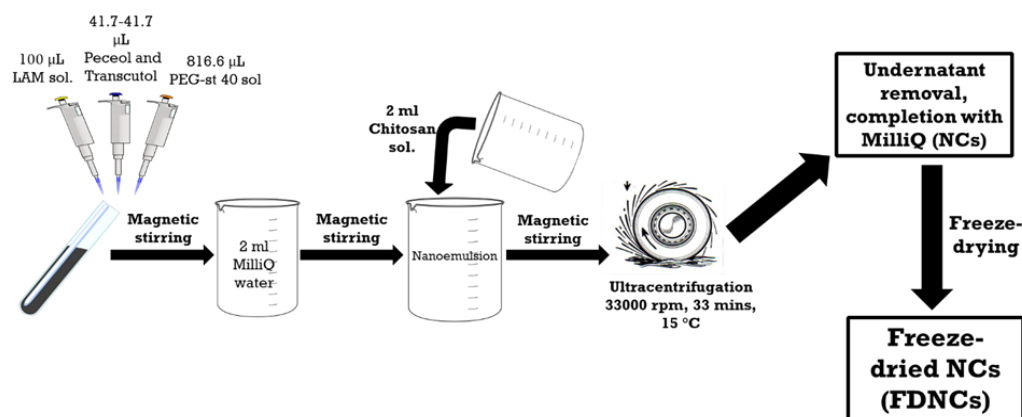


**Figure 6.** The process of NC and FDNC preparation

#### 4.2.6. Micrometric investigation methods

##### *Determination of particle size of NP formulation*

The particle size of the microparticles was characterized by using Leica Image Processing and Analysis System device (Leica Q500MC; Leica Microsystems, Wetzlar, Germany). The test parameters of 300 particles were their length, width, area, and district/convex perimeter.

The particle size of the LAM nanoparticles – the particles were on the surface of the polymer microparticles – were investigated by SEM pictures (Hitachi S4700; Hitachi Ltd., Tokyo, Japan) at 10 kV. The distribution of LAM particle diameter was obtained by analyzing SEM images with the ImageJ software (1.50i; Java 1.6.0\_20 [32-bit]; Windows NT) environment using approximately 500 particles.

##### *Particle size, particle size distribution and surface charge characterization of NCs*

The particle size and polydispersity index of the NCs were determined by photon correlation spectroscopy (PCS) (Zetasizer NanoZS<sup>®</sup>, Malvern Instruments; Malvern, United Kingdom). In the case of surface charge, zeta potential (ZP) measurements were done by laser Doppler anemometry (LDA) using the same equipment. All the measurements were performed at 25 °C with a detection angle of 173° in distilled water unless otherwise indicated. The freeze-dried NCs were investigated with the same instrument after redispersion with MilliQ water. The FDNCs samples were investigated after resuspension in MilliQ water.

##### *Image analysis (SEM)*

The morphology of particles was investigated by SEM (Hitachi S4700; Hitachi Ltd., Tokyo, Japan) at 10 kV. The samples were gold–palladium-coated (90 s) with a sputter coater (Bio-Rad SC502; VG Microtech, Uckfield, UK) using an electric potential of 2.0 kV at 10 mA for 10 min. The air pressure was 1.3–13.0 mPa.

#### 4.2.7. Structural investigations

##### *Differential scanning calorimetry (DSC)*

The thermal response of each product was measured using a differential scanning calorimeter (Mettler Toledo TG 821<sup>e</sup> DSC; Mettler Inc., Schwerzenbach, Switzerland). About 3–5 mg of powder was precisely weighed into DSC sample pans, which were hermetically sealed, and the lid was pierced. Each sample was measured in the temperature interval of 25–230 °C at a heating rate of 5 °C/min and under a constant argon flow of 150 mL/min. Data analysis was performed using the STAR<sup>e</sup> software (Mettler Toledo; Mettler Inc., Schwerzenbach, Switzerland). The crystallinity index was calculated based on the normalized integral values. PM samples were regarded as 100%.

##### *X-ray powder diffraction (XRPD)*

The XRPD measurement was carried out with a BRUKER D8 advance X-ray powder diffractometer (Bruker AXS GmbH, Karlsruhe, Germany) with Cu·K  $\lambda$ I radiation ( $\lambda=1.5406$  Å) and a VÅNTEC-1 detector (Bruker AXS GmbH, Karlsruhe, Germany). The powder samples were loaded in contact with a plane quartz glass sample slide with an etched square and measured. Samples were scanned at 40 kV and 40 mA. The angular range was 3–40° 2 $\theta$ , at a step time of 0.1 seconds and a step size of 0.007°. All manipulations, including K $\alpha$ 2 stripping, background removal and smoothing of the area under the peaks of the diffractograms, were performed using the DIFFRACplus EVA software. The crystallinity index ( $X_c$ ) values were calculated based on the following formula (Equation 1.), where A marks the area under the whole curve:

$$X_c = \frac{A_{crystalline}}{A_{crystalline} + A_{amorphous}} * 100$$

PM samples were regarded as 100%.

#### 4.2.8. *In vitro* studies

##### *Encapsulation efficacy (EE) and drug loading (DL) of NCs*

After centrifugation, the supernatant was analyzed for the amount of drug present with a UV spectrophotometer (Synergy<sup>TM</sup> H1 Microplate Reader, BioTek Instruments, Inc.) at  $\lambda_{max}$  of 307 nm after suitable dilution. EE% was calculated by the following equation (Equation 2.):

$$\%EE = ((W_1 - W_2) / W_1) * 100$$

Loading capacity (percentage drug loading [%DL]) was calculated by Equation 3.:

$$\%DL = ((W_1 - W_2) / (W_1 - W_2 + W_{lipid})) * 100$$

where,  $W_1$ ,  $W_2$ , and  $W_{lipid}$  are the weight of drug added to the formulation, the analyzed weight of the drug in the supernatant, and the weight of the lipid added to the formulation, respectively.

### ***In vitro release study of nasal powders***

The modified paddle method (USP dissolution apparatus, type II; Pharma Test, Hainburg, Germany) was used to examine the dissolution rate of the samples and determine their drug release profile. The tests were carried out under nasal conditions for temperature and pH. 100 mL phosphate-buffered saline solution (PBS of pH 5.60 at 30 °C) was used as a medium, in which 108 mg of the samples were tested in case of nasal powders. The paddle was rotated at 50 rpm, and the sampling points were at 5 min, 10 min, 15 min, 30 min, and 60 min. In the beginning, the sampling point was more frequent, because the beginning of the investigation is more important as the mucociliary clearance renews the mucus every 15 min. The following sampling points offered extra information about the dissolution behavior of LAM. After filtration, the drug content of the aliquots was determined using spectrophotometry (Unicam UV/VIS Spectrophotometer, Cambridge, UK) at 307 nm. The tests were carried out in triplicates.

### ***In vitro release study of NCs***

The modified paddle method (USP dissolution apparatus, type II; Pharma Test, Hainburg, Germany) was used to examine the dissolution rate of NCs and determine the drug release profile from the samples. To model the nasal pH and temperature conditions, the medium was 9 mL phosphate-buffered saline (PBS) adjusted to pH 5.60. Samples with 1,65 mg LAM were tested in this medium at 30 °C with paddle stirring at 50 rpm. The sampling points were at 5 min, 10 min, 15 min, 30 min, 45 min, and 60 min. The first data points were considered the most important as the mucociliary clearance renews the mucus every 15 min. The following data points offered additional information about the dissolution behavior of LAM. The samples were investigated with an RP-HPLC-DAD system. The RP-HPLC-DAD consisted of an Agilent 1200 Series chromatograph and a DAD detector. The stationary phase was a Kinetex<sup>®</sup> C<sub>18</sub> columna (150 mm x 4,6 mm, particle size: 5 µm, pore diameter size: 100 Å). The separation was isocratic, the composition of the mobile phase was 0,01 M phosphate buffer (pH= 6,7 ±0,1): methanol:acetonitrile = 50:20:30 (v/v). The analytical column was tempered for 25 °C and the measurements lasted 10 mins. The flow rate was 0.75 mL/min, and 10 µL of the sample was injected into the flowing fluid, measured at 307 nm. The equation for the calibration line was  $y = 12,335x - 3,488$  ( $R^2=1$ ). The equation was valid in the range of 10-150 µg/mL. The tests were carried out in triplicates.

#### ***4.2.8.1. Development of in vitro permeability investigation method***

##### ***Horizontal diffusion studies***

A horizontal diffusion device (Side-Bi-Side<sup>™</sup> Crown Glass, USA) was used for the investigation of NPs and the tests were carried out under nasal conditions. Regenerated



cellulose membrane (Whatman™) with 0.45 μm pore diameter was soaked in IPM, and the donor phase was tempered to 30 °C at pH 5.6. The acceptor phase was pH 7.4, and the content of the diffused drug was measured spectrophotometrically at 307 nm (Unicam UV/Vis Spectrophotometer, Cambridge, UK).

### *The execution of diffusion measurements*

Then we aimed to develop the above-mentioned method, the same device (Figure 7.) was investigated and used to optimize a method proper for API-investigations comprising different logP values. The factors listed on the Ishikawa diagram influence the efficiency of *in vitro* membrane diffusion in different extent. The modification consisted of the change in the volume of the chambers (from 3 mL to 9 mL), the arrangement of the space for the magnetic stirrers, the design of probe input for real-time analysis, membrane surface with a small area. This device consists of two chambers: a donor and an acceptor phase with a horizontal orientation. Our donor and acceptor phases were 9 mL. The volume of the nasal cavity is 15-20 mL which is divided by the nasal septum into fossae, therefore 9 mL was the ideal choice to model the absorption in the nasal fossa. The temperature was set at 30 °C suiting the average temperature of the human nose. The rotational speed of magnetic stirrers was around 100 rpm.

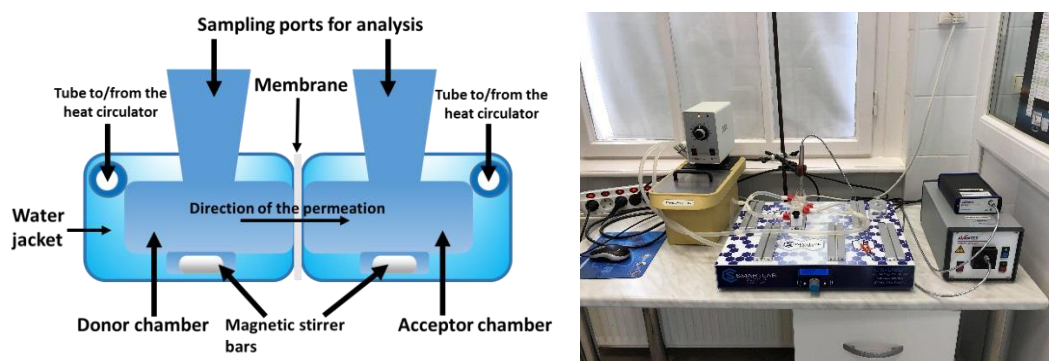


**Figure 7.** The setup of the horizontal device used for *in vitro* modeling of the penetration of the nasal powders

Three types of membrane (Metricel®, Isopore™ or Whatman™) were chosen and isopropyl myristate was used as an impregnation agent to imitate the hydrophobic property of the wall of the nasal epithelial cells, reference was a PBS (pH=7.4). 10±0.50 mg powder of APIs (MEL, LAM, LEV) was weighted and the results were corrected depending on the actual weight because the human nose can accommodate around 10-25 mg powder *per nostril per shot* [21]. The penetration extent ( $P_{API}$ , μg/cm<sup>2</sup>) can be used in the case of nasal formulations to describe the extent of diffusion. In spite of that, thanks to the mucociliary clearance, the residence time of the nasal formulations are around 15 min on the nasal mucosa, the measurements lasted for 60 min so that the kinetics could be better characterized.

The diffusion surface was 0.785 cm<sup>2</sup>. The area of nasal mucosa in the human body is around 200 times larger: 160 cm<sup>2</sup> [103], therefore presumably multiple times more API would be supposed to be penetrated (Equation 4.) *in vivo* than in the horizontal device.

$$P_{API} = \frac{\text{Mass of permeated API } (\mu\text{g})}{\text{Diffusion surface } (\text{cm}^2)}$$

The MEL was quantified at 366 nm, LAM: at 307 nm, LEV: 281 nm.

#### ***Offline spectrophotometric measurements***

At determined moments (5, 10, 15, 30, 45 and 60 min), 2 mL samples were taken from the acceptor phase and the volume was made up to 10 mL, therefore the acceptor phase was diluted after every occasion. The dissolved drug amount was determined spectrophotometrically (PerkinElmer, Lambda 20 spectrophotometer, Dreieich, Germany). The path length was 1 cm. Flux (J) and permeability coefficient (K<sub>p</sub>) values were calculated according to the following formulas (Equation 5. and 6.):

$$J = m / (A * t)$$

$$K_p = J / c_d$$

where m is the amount of diffused LAM, A is the surface of the membrane, t is the time and c<sub>d</sub> is the concentration of LAM in the donor phase.

#### ***Inline measurements with a probe connected with an optical fiber to a spectrophotometer***

An AvaLight DH-S-BAL spectrophotometer (AVANTES, Apeldoorn, Netherlands) was connected to an AvaSpec-2048L transmission immersion probe (AVANTES, Apeldoorn, Netherlands) with optical fiber to quantify the amount of the API. The path length was 1 cm. The limiting factor of inline measurements can be that no dilution occurs in the acceptor phase during the measurements which could model the dilution happening in the blood by transferring the API from the direct environment of the nose [104].

#### ***Application of modified permeability investigation method***

As for the LAM measurements, the arithmetic mean of the Metrical<sup>®</sup> membrane was a bit lower compared to Whatman<sup>™</sup>, the higher extent of penetration was in favor of the use of Whatman<sup>™</sup> in inline measurements when the impregnation agent was IPM. In the case of IPM impregnation, the inline measurements were more precise than the offline ones, therefore, they are suggested. This means that the previously used method and parameters were the most suitable for LAM and, therefore, the NCs were measured with the same method like the NPs were, but with AvaLight DH-S-BAL spectrophotometer (AVANTES, Apeldoorn, Netherlands) connected to an AvaSpec-2048L transmission immersion probe (AVANTES, Apeldoorn, Netherlands) with optical fiber to quantify the amount of API. The path length was 1 cm. The NPs were remeasured with the inline method and there was no

significant difference in the results, so we decided to use the original data, but we were able to set up a new method, which is easy to implement, more accurate, more reproducible, which made our experiments more simple and more effective.

#### **4.2.9. *In vivo* studies**

##### ***Intranasal administration, blood sample collection, and brain removal***

The nanoLAM powder and also the PM contained 0.555 mg, while the NC formulation contained 0.066 mg LAM and the FDNCs formulation contained 0.039 mg LAM. The doses were the maximums that a rat nostril can tolerate and we were able to administer. The formulations were administered into the right nostril of 160–180 g male Sprague–Dawley rats (n=4) with a small spatula or pipette. The administration was carried out under isoflurane short anesthesia. As a control, IV injections of LAM solutions (IV LAM), which contained 0.555 mg of API were given to rats (n=4). At predetermined time points (3, 6, 10, 20, 40 and 60 minutes) after LAM administration, blood samples were collected by cardiac puncture into heparinized tubes under deep isoflurane anesthesia. Then the animals were sacrificed by decapitation, and brain tissues were quickly removed, rinsed in ice-cold PBS, divided into left and right hemispheres, weighed, and stored at -80 °C until assayed. The experiments were performed according to the EU Directive 2010/63/EU for animal experiments and were approved by the Hungarian Ethical Committee for Animal Research (permission number: IV/1247/2017).

##### ***Plasma sample preparation***

To 100 µL of plasma samples 20 µL internal standard solution (0.4 µg/mL, lamotrigine-13C<sub>3</sub>, d<sub>3</sub> in methanol-water, 50:50, v/v), 20 µL methanol-water mixture (50:50, v/v) and 100 µL 2M sodium hydroxide were pipetted, and the samples were vortexed. For the liquid-liquid extraction, 1 mL ethyl acetate was added to each tube and vortexed for 1 min, shaken at room temperature for 10 min and left on ice for 5 min. After centrifugation, 300 µL of the supernatant was transferred to a 1.5 mL glass vial and evaporated to dryness at room temperature using a gentle stream of nitrogen. The samples were resuspended in 50 µL of acetonitrile containing formic acid (0.1% v/v) and diluted with 0.1% formic acid to a final volume of 400 µL. 20 µL was injected into the LC-MS/MS system for analysis.

Prior to the extraction of the calibration and quality control samples, 20 µL of a standard solution (6.25 ng/mL – 8 µg/mL LAM) was added to LAM-free pooled rat plasma instead of a methanol-water mixture. The rest of the sample preparation steps were the same as described above.

### ***Brain tissue sample preparation***

Brain samples were homogenized in water (4 mL/g wet tissue weight) on ice 2 times for 30 seconds with an ULTRA-TURRAX blade-type homogenizer (IKA<sup>®</sup> Works, Inc; Wilmington, USA) and for 30 seconds with a BioLogics Model 150VT ultrasonic homogenizer (BioLogics Inc, Manassas, USA). The samples thus prepared were stored at -80 °C until use. On the day of extraction the samples were thawed, and to 200 µL brain homogenates 20 µL internal standard solution (0.5 µg/mL, lamotrigine-13C<sub>3</sub>, d<sub>3</sub> in methanol-water, 50:50, v/v), 20 µL methanol-water mixture (50:50, v/v) and 20 µL 20% (w/v) trichloroacetic acid (TCA) were added. Samples were vortexed and centrifuged with 10,000 x g at 20 °C for 10 minutes and then 100 µL of the supernatant was placed to a new test tube. LAM was extracted after adding 100 µL 4M sodium hydroxide and 1 mL ethyl acetate, by vortexing for 1 min, shaking at room temperature for 10 min and resting on ice for 5 min. After centrifugation, 700 µL of the supernatant was transferred to a 1.5 mL glass vial then evaporated to dryness at room temperature. The samples were resuspended in 50 µL of acetonitrile containing formic acid (0.1% v/v), diluted with 0.1 % formic acid to a final volume of 370 µL and than 20 µL was injected into the LC-MS/MS system for analysis.

Prior to the extraction of the calibration and quality control samples, 20 µL of a standard solution (7.8125 ng/mL - 10 µg/mL LAM) was added to the pooled LAM-free rat brain homogenate instead of a methanol-water mixture. Further sample preparation steps were the same as described above.

### ***LC-MS/MS***

The liquid chromatographic separation was performed on an Agilent 1100 Series HPLC system (Agilent; Santa Clara, USA) using a Kinetex C18 (2.6 µm 100A, 50 x 2.1 mm) column (Phenomenex; Torrance, USA). In front of the analytical column, a C18 guard column was used. Water (A) and acetonitrile (B) both containing formic acid (0.1% v/v) were used as mobile phases. A gradient elution program was used to elute components: gradient started at 13% B, increased linearly to 90% B in 3 min, kept at 90% B for 2 min, dropped back to 13% B in 0.1 min and kept at 13% B for 2.9 min. The flow rate was set at 300 µL/min for the separation and 500 µL/min to wash and equilibrate the column. The autosampler and the column were maintained at room temperature.

Samples were analyzed with an on-line connected Q Exactive Plus quadrupole-orbitrap hybrid mass spectrometer (Thermo Fisher Scientific; Waltham, USA) equipped with a heated electrospray ion source (HESI). It operated in positive mode with the following conditions: capillary temperature 256 °C, S-Lens RF level 50, spray voltage 3.5 kV, sheath gas flow 48, sweep gas flow 2 and auxiliary gas flow 11. The automatic gain control (AGC) setting was defined as  $2 \times 10^5$  charges and the maximum injection time was set to 100 ms. Collision

energy (CE) was optimized and set at 31 eV for LAM and lamotrigine-13C3, d3 (ISTD). The precursor to product ion transition of m/z 256.01 → 108.98 (qualifier), 256.01 → 210.98 (quantifier) for LAM and m/z 262.04 → 110.99 (qualifier), 262.04 → 217.01 (quantifier) for ISTD were used for parallel reaction monitoring (PRM).

Data acquisition and processing were performed using Xcalibur™ and Quan Browser softwares (Thermo Fisher Scientific; Waltham, USA).

#### ***Calculation of drug targeting efficiency***

Drug targeting efficiency (DTE) – relative exposure of the brain to the drug following intranasal administration vs. systemic administration – was calculated according to the following formula (Equation 7.):

$$DTE = \frac{\left(\frac{AUC_{brain}}{AUC_{blood}}\right)_{IN}}{\left(\frac{AUC_{brain}}{AUC_{blood}}\right)_{IV}}$$

The value of DTE can range from  $-\infty$  to  $\infty$ , and the values higher than 1.0 indicate more efficient drug delivery to the brain following intranasal administration as compared to the systemic administration [105].

#### ***Calculations of the area under the time-concentration curve (AUC) and statistical analysis***

The calculation of area under the curve (AUC) of the time (min) – concentration ( $\mu\text{g/L}$ ) curves of each group of animals were performed with the PKSolver add-in from Microsoft Excel (MS Office 2010) using the non-compartmental analysis of data after extravascular input (model #101) of LAM [106]. The AUC values were calculated using the linear trapezoidal method. Because of the incomplete elimination of LAM, the following parameters were not determined:  $\lambda$ ,  $t_{1/2}$ ,  $AUC_{0-\infty}$ ,  $AUMC_{0-\infty}$ ,  $V_d$ , and  $Cl$ . All reported data are means  $\pm$  SD.

#### **4.2.10. Stability measurements**

Stability tests of NPs were performed in Binder KBF 240 (Binder GmbH, Tuttlingen, Germany) equipment, with a constant-climate chamber. An electronically controlled APT.line™ line preheating chamber and refrigerating system ensured temperature accuracy and reproducibility of the results in the temperature range between 10 and 70 °C and the relative humidity (RH) range between 10 and 80%. The stability test was performed at  $25 \pm 2$  °C with  $50 \pm 5\%$  RH (room conditions). Sampling was carried out after 1 day; 3 and 6 months.

Statistical analysis was performed with TIBCO Statistica® 13.4 (Statsoft Hungary, Budapest, Hungary). All reported data are means  $\pm$  SD. The Student's t-test was used to determine the statistical significance. Changes were considered statistically significant at  $p < 0.05$ .

## 5. RESULTS AND DISCUSSION

### 5.1. Development of NP formulation

#### 5.1.1. Knowledge space development and RA

The first step was setting up an Ishikawa (fishbone) diagram including all the parameters influencing the desired NP product containing LAM as the active agent. The parameters were ranked into four groups (Figure 8.), namely, 1) material characteristics; 2) production method; 3) product characteristics and 4) therapeutical expectations. This process gave a collection of preliminary knowledge and information, which helped to design the experiments and to select the appropriate CQAs and CPPs of the drug development procedure.

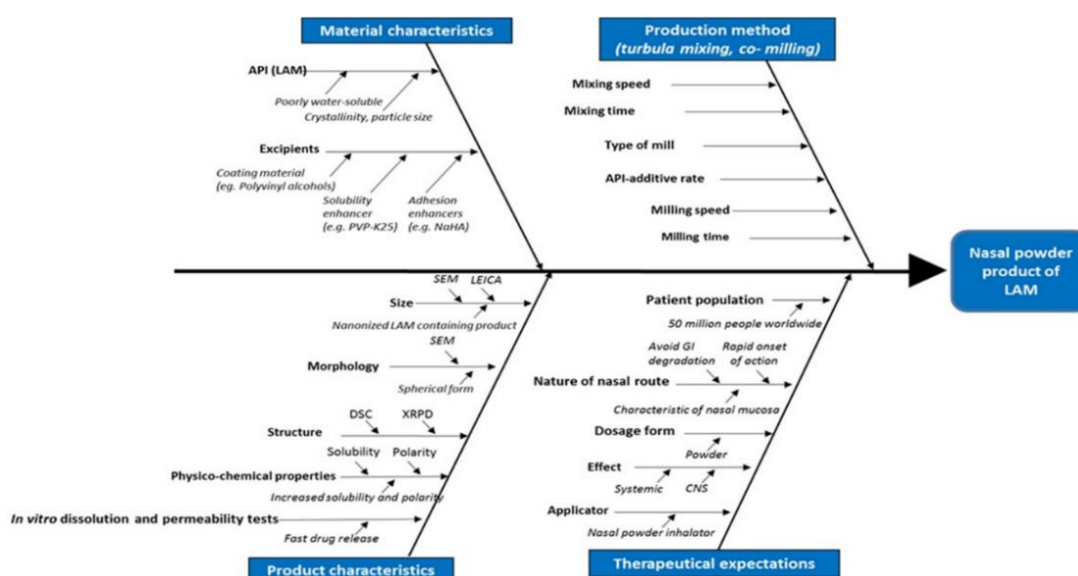


**Figure 8.** Ishikawa diagram illustrating the parameters influencing the quality of the nanonized LAM containing NP product [82]

First of all, the QTPP that describe the desired NP, which contain the nanosized LAM, were defined, and the CQAs and the CPPs were also identified. The results of the interdependence rating made by the research group members and the selected target and critical parameters are presented in the tables of Figure 9. Below them, Pareto charts can be seen, as the result of the RA generated by the software. The Pareto charts show the relative effect of the CQAs and the CPPs on the QTPP, namely, the numeric data of the critical factors and their ranking. In the diagrams, the same colors were used as in the tables; the factors that have minimal effect on the final product quality were marked with green, the factors with the medium effect were marked with yellow and the factors with great impact were marked with red. As a result, it was found that theoretically among the CQAs, the particle size and its distribution can be predicted to have the greatest effect on the quality of the targeted and desired NP product. The analog diagram shows that among the CPPs, milling time and speed had to be expected to have the highest influence on the quality of the aimed product (Figure 9.). According to the RA results, the studies of the practical development (screening studies and product preparation) were focused on the selected CQAs (particle size and distribution of LAM and

dissolution, as investigated outputs) and CPPs (milling time, milling speed and the API: additive ratio).

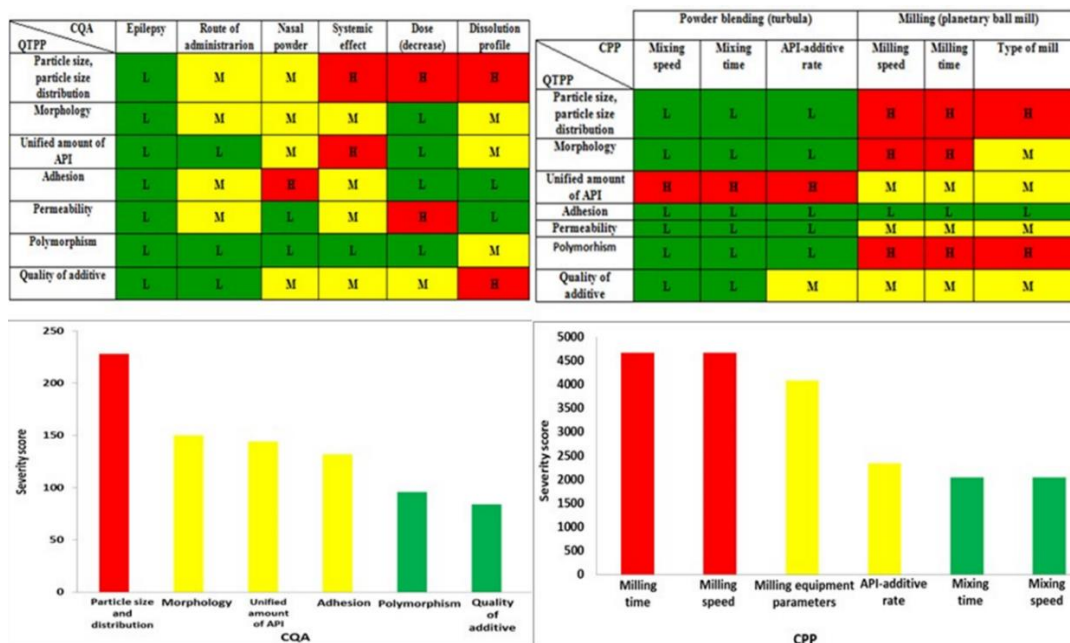


**Figure 9.** Results of the interdependence ratings of the QTPP and CQA and of the CPP (upper parts) and the Pareto charts of the CQA and CPP with calculated numeric severity scores (lower parts) generated by the RA software [82]

According to the results of the initial RA, the ratio of API and additives was found to be critical. In this meaning, in all additives, a ratio of 1:1 was selected for production; the milling time and milling speed were also constant, and the LAM size in the product, distribution, and dissolution as responses were investigated afterward.

Preliminary experiments were carried out to collect information about the impact of grinding on raw materials (LAM and excipients) especially on micrometric properties and their structure. They were required because adhesion, aggregation, and amorphization may occur due to grinding. The raw materials were milled for 2 hours on 400 rpm.

## 5.1.2. Investigation of NP formulations

### 5.1.2.1. Micrometric properties

#### Particle size analysis

The particle size of the co-milled samples (Table 5.) was 10–25  $\mu\text{m}$ , which is in the desired range. The particles are small enough to reach the nasal mucosa but not too small to be inhaled into the lungs. The smallest particle size was measured for the powder containing PVP and the largest one for the sample that contained PVA, particle size of which hardly decreased. In the table, it can also be seen that the particle size of LAM was between 120 and 230 nm; it is in the target range. Compared to PM samples, it can be observed that in all three cases, the polymers could prevent the adhesion of the LAM particles, while the particle size of the polymers and LAM decreased due to co-milling, mostly in the samples that contained NaHA.

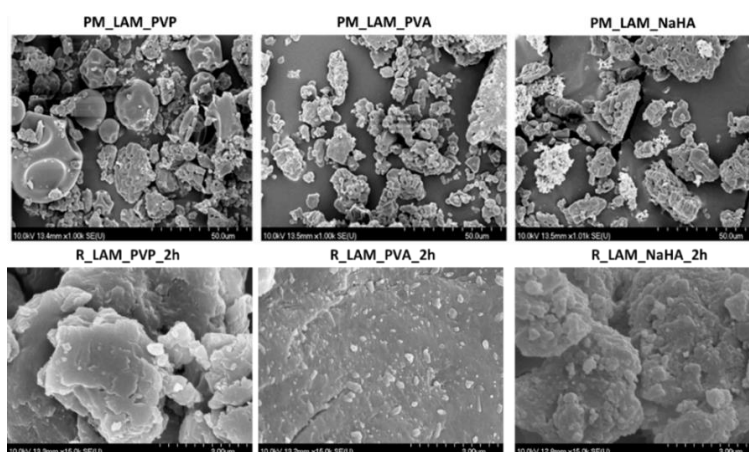


**Table 5.** The particle size of PM and co-milled (marked with R) samples

	Length ( $\mu\text{m}$ )	Width ( $\mu\text{m}$ )	Average particle size of LAM ( $\mu\text{m}$ )
PM_LAM_PVP	26.80	18.96	$7.63 \pm 20.07$
R_LAM_PVP	13.60	9.06	$0.121 \pm 0.027$
PM_LAM_PVA	26.90	17.05	$13.88 \pm 21.15$
R_LAM_PVA	25.33	16.61	$0.15 \pm 0.042$
PM_LAM_NaHA	37.07	18.75	$26.17 \pm 27.68$
R_LAM_NaHA	16.83	11.30	$0.23 \pm 0.016$

### *Particle size and morphology (SEM)*

Figure 10. shows the SEM pictures of the samples. It can be seen that LAM particles aggregated in the case of PM samples, which explains the large particle size. On the other hand, LAM particles adhered to the surface of the polymers and their size was in the nano range. In the case of the PVA-containing sample, uniformly dispersed, non-aggregated LAM particles can be observed as well. The increase in the temperature level due to grinding ( $30\text{ }^{\circ}\text{C}$ – $36\text{ }^{\circ}\text{C}$ ) was not high enough to reach the glass transition temperature of the polymers (PVP:  $130\text{ }^{\circ}\text{C}$ , PVA:  $80\text{ }^{\circ}\text{C}$ , NaHA:  $244\text{ }^{\circ}\text{C}$ ); hence, as a result, no relevant change occurred. It can be concluded that the applied polymers offer great matrix to the LAM particles, where their individuality and stability, which have a great influence on the dissolution, are ensured.

**Figure 10.** Particle morphology of PM and co-milled samples [82].

#### *5.1.2.2. Structural investigations*

Generally, it can be said that the intensity of the peaks in XRPD diffractograms decreased in each co-milled sample due to the effect of milling and the presence of adjuvants, which indicates a reduced degree of crystallinity. In the product, which contained PVP and PVA, the nearly amorphous polymer covers the crystalline LAM; thus, the characteristic  $2\theta$  values are not visible on the chart compared to the PM. When the sample contained NaHA, the amorphous property of the polymer is more dominant; therefore, the characteristic peaks of the active substance are present; however, their intensity is not so high as in the case of the PM (Figure 11. A).

On the DSC curves (Figure 11. B) of the sample which contained LAM and PVP, no endothermic peak can be detected because the particles merged into the polymer particles. In



the case of the NaHA containing product, the melting point was not significantly different from the one in the case of the PM, but the sample that contained PVA showed a significant decrease in melting point.

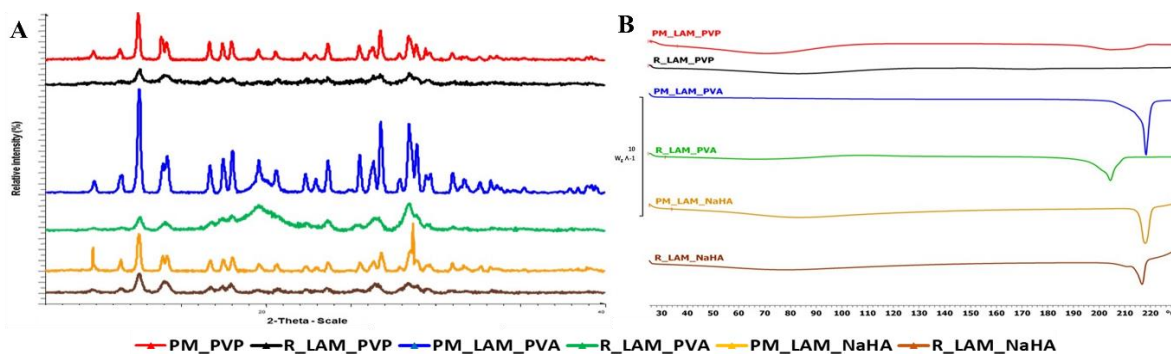


**Figure 11.** XRPD diffractograms (A) and DSC curves (B) of co-milled (marked with R) and PM samples

The crystallinity index values were calculated after the investigation of the DSC curves and the XRPD diffractograms to reveal changes in the degree of crystallinity in the milled samples compared to the PMs (Table 6.). It can be seen that the values are correlating, as similar results were obtained in both cases when the samples contained PVA or NaHA. In the case of the samples that contained PVP, the polymer-coated the LAM crystals and at the same time protected them from amorphization. That is why no peak can be seen in the DSC curve, but the crystallinity index increased based on the XRPD diffractograms.

**Table 6.** Calculated crystallinity indexes of co-milled (marked with R) samples after DSC and XRPD measurements compared to PM samples

	$X_c$ (%)	
	XRPD	DSC
R_LAM_PVA	67.42	74.45
R_LAM_PVP	70.84	-
R_LAM_NaHA	46.76	50.06

### 5.1.2.3. Dissolution and permeability tests of the samples

In the case of the *in vitro* (Figure 12.) investigations, it can be generally said that the co-milled samples performed much better than the PMs. This means that higher dissolution (Figure 12. A) and permeability rates (Figure 12. B) were detected during the tests when LAM was co-milled with adjuvants. Especially the sample, which contained PVA, showed really high values as the percentage of dissolved LAM was 100% after 5 minutes and the highest LAM concentration in the acceptor phase was detected after 60 minutes. These results mean that the application of this formulation can lead to a rapid onset of action and sufficient LAM amount in the CNS, thus we used PVA as an adjuvant hereinafter.

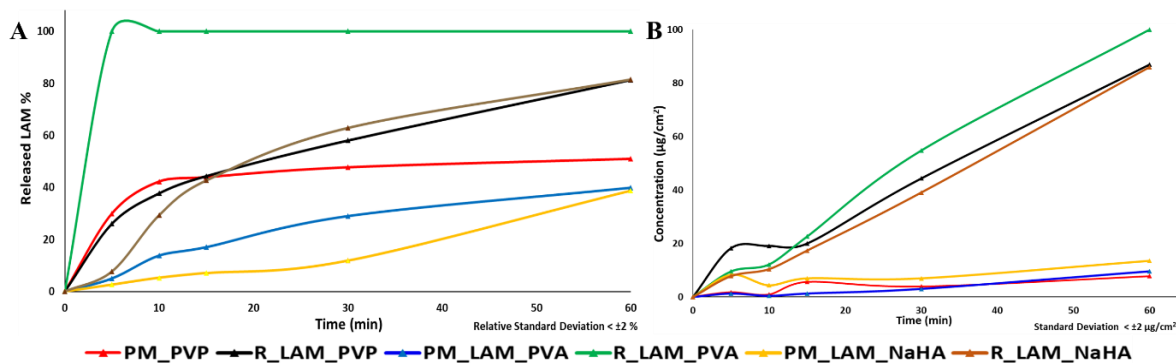


**Figure 12.** Dissolution curves (A) and permeability profiles (B) of the PM and co-milled (R) samples Table 7. shows the calculated flux and permeability coefficient values. It can be seen that the values of PMs are lower than the values of the co-milled samples. The sample containing PVA had the best permeability as the highest concentration of LAM was detected in the acceptor phase after 60 minutes. The reason for this high permeability can be explained by the function of PVA, which can preserve the uniqueness of the particles, and the liberation of nanoparticles. The liberation increases the diffusion pressure due to the increased concentration gradient. In the case of PVA and NaHA, there was no considerable difference.

**Table 7.** Calculated Flux and permeability values. Co-milled samples are marked with R.

	<b>J [<math>\mu\text{g}/\text{cm}^2/\text{h}</math>]</b>	<b>K<sub>p</sub> [cm/h]</b>
<b>PM_LAM_PVP</b>	7.82	0.0026
<b>R-LAM_PVP</b>	86.95	0.0261
<b>PM_LAM_PVA</b>	9.56	0.0031
<b>R-LAM_PVA</b>	100.00	0.0300
<b>PM_LAM_NaHA</b>	13.47	0.0044
<b>R-LAM_NaHA</b>	86.08	0.0259

### 5.1.3. Definition and validation of the Design Space of the NP samples

Our aim afterward was to identify the DS by optimizing the parameters of the dry milling method. The parameters were chosen according to previously discussed investigations. DS also allows to secure the quality of our samples and helps to find the optimal formulation for producing nasal powder formulation containing nanonized LAM particles. As the use of PVA was really promising, it was chosen as a hydrophilic matrix polymer to prevent the nanoparticles from aggregation [32].

#### *Experimental plan and proven acceptable range (PAR) determination*

As it had been determined previously, there are 3 main CPPs (milling time and speed, LAM:PVA ratio). The software recommended a 3<sup>3</sup> factorial experimental plan. The PAR, which was generated by the MODDE 11.1 software, is ‘a characterized range of a process parameter for which operation within this range, while keeping other parameters constant, will result in producing a material meeting relevant quality criteria’, according to the ICH Q8 guideline. Table 8. shows the factors and their variation levels along with the chosen responses and their values, and also indicates the PAR of all responses.

**Table 8.** The parameters of milling, the chosen responses, and their values

Name	Settings	Name	Min	Max	Target
Milling time (h)- X1	0.5, 1, 2	Mean size of LAM -Y1		250 nm	350 nm
Milling speed (rpm)- X2	200, 300, 400	Standard Deviation -Y2		±100 nm	±200 nm
PVA:LAM (m/m%)- X3	0.5, 0.75, 1	Released LAM % after 5 mins -Y3	70%		85%
		Released LAM % after 10 mins -Y4	85%		100%

***DoE analysis, summary of fit***

It can be observed that the high milling time, speed and LAM:PVA ratio do not always result in small particle size and standard deviation, and high dissolved amount of LAM. To check the validity of the experimental design, the following statistical parameters were determined:  $R^2$ ,  $Q^2$ , model validity, and reproducibility. The values of these parameters are presented in Table 8. All responses were fitted and well predicted by the model as  $R^2$  values were at least 0.8 and all the  $Q^2$  values were above 0.5. The validity value of the models was above 0.25 in each case, which indicates a good model. The reproducibility values also presume that the process is well-reproducible as they were above 0.9. Model significance test using ANOVA generated lower 0.05 p values for all responses. Also, there was no lack of fit detected, as the model error was not significantly different from the replicate error ( $p > 0.05$ ) (Table 9.).

**Table 9.** Summary of fit for DoE, ANOVA Test results for model significance and lack of fit (p values)

Response	$R^2$	$Q^2$	Validity	Reproducibility	Model Significance	Lack of fit test
Y1	0.82	0.64	0.34	0.96	5.57E-06	0.073
Y2	0.88	0.72	0.28	0.97	8.19E-07	0.057
Y3	0.80	0.70	0.49	0.94	4.82E-08	0.285
Y4	0.87	0.77	0.69	0.91	1.15E-08	0.115

***Effect of the milling parameters on the responses***

After the evaluation of the coefficient plots (Figure 13.), it can be seen that milling time and speed have an effect on Y1. As the milling time and speed increase, the particle size of the API decreases, so it can be concluded that these parameters influence mostly Y1 and Y2. The values of LAM size were between 172 nm and 7015 nm. There were some samples, where due to the inappropriate parameters the particles aggregated, which means that the detection of unique particles was not possible. The same phenomenon was observed in the case of Y2. The increasing milling time and speed decreased Y2. This is related to the smaller particle size because the particles became more unique (no aggregation occurred), so the particle size determination was simpler above certain parameter values. In the coefficient plot of SD, a significant interaction could be observed, but its interpretation is possible after the examination of the surface plots. The Y3 and Y4 values increased due to the increased values of the milling parameters. The reason for this tendency is that the small particles can leave the

matrix easier than bigger ones, and also due to reduced particle size, the bigger surface is advantageous if the aim is rapid dissolution. However, in these cases, the PVA:LAM ratio has an effect on the dissolution rate due to the matrix effect of the polymer. A quadratic term between milling time is also observed in the coefficient plots.

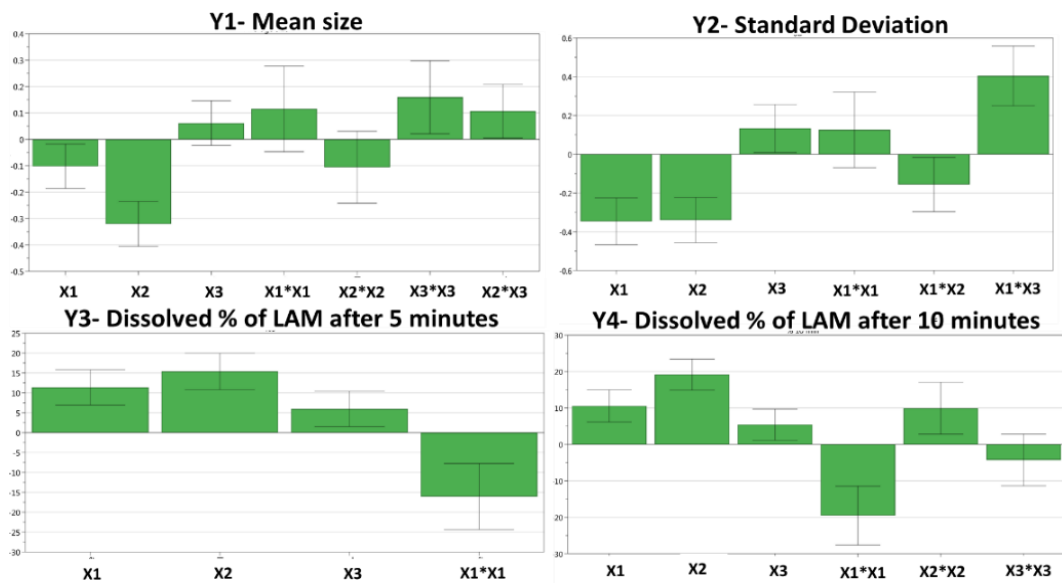


**Figure 13.** The scaled and centered coefficient plots of the responses, where X1: milling time; X2: milling speed; X3: PVA: LAM (m/m%) ratio (X3) [83]

### *Design Space estimation*

The major objectives of QbD are risk minimization and DS development for the product. Design Space plots are generated by superimposing several contour plots and combining it with probability analysis [96,98,100]. Considering the models developed for the CQAs, Monte Carlo simulations were used to estimate the probability to meet the product specifications in the design region. The plot is a color-coded region and contour lines, which have the role to separate the design region according to the probability of failure, are expressed in percentage (%) of failure. The green region, with a low probability of failure, is named the DS. The edges of the hypercube illustrate the generated PAR. The milling time was between 1.4 h and 1.7 h, while the PVA:LAM ratio was between 0.77 and 0.83. The milling speed was kept constantly high, on 400 rpm as it had the narrowest variation range among the input variables, and it had the highest influence on the responses according to the coefficient plots. The target values can be achieved using parameters in these ranges that are near to 0 levels in Table 8. MODDE can calculate a setpoint after running the optimizer that can estimate the tolerance available for the factors. During the setpoint analysis, a robustness estimate is calculated by adding disturbances to the factors around the setpoint. In our study, it was also our aim to find a robust setpoint. It is a solution with maximum factor ranges that will predict results inside the specifications. The robust setpoint is the center of the green region which is 1.5 h milling time with 0.8 PVA:LAM ratio on 400 rpm speed (Figure 14.) in our case.

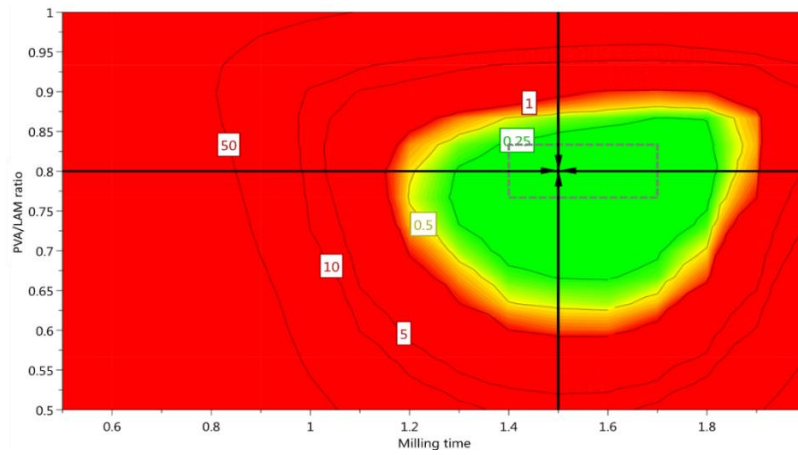


**Figure 14.** The Design Space of the dry milling method. The edges of the hypercube are between 1.4 h and 1.7 h in the case of milling time, 0.77 and 0.83 in the case of the PVA: LAM ratio, respectively. Milling speed is kept constantly 400 rpm. The parameters of the robust setpoint are 1.5 h, 400 rpm, and 0.8 PVA:LAM ratio [83]

### *Validation of the Design Space*

As there are infinite good formulations, it seemed to be the most rational to keep the PVA:LAM ratio at the robust setpoint. Milling speed was kept at 400 rpm because the interval was narrow and lower speeds were not adequate. In our previous study, the milling time was 2 hours, but we aimed to rationalize the processing time. After the evaluation of the results of nanoLAMpowder – that was prepared according to the robust setpoint and the results which had been proven to be good – it would have been irrational to use longer milling times. That is why milling time was no longer than 1.5 hours. The regions of the DS were expressed in % of failure, the validation process of the DS based on these regions. The first sample was prepared outside the 50% probability of failure (P1), the second was in the region of 50% probability of failure (P2), the third was in the near edge of 10% probability of failure (P3), the fourth was in the region of 5% probability of failure (P4), the fifth was in the near edge of 1% probability of failure (P5), the sixth was inside the region of 0.5% probability of failure (P6), and the last one was prepared according to the robust setpoint (P7- nanoLAMpowder). Validation samples were prepared with PVA:LAM ratio of 0.8 on 400 rpm and by using different milling times, that was varied according to Table 10.

**Table 10.** The experimental plan of Design Space validation

Sample	Milling time (h)	Milling speed (rpm)	PVA: LAM ratio (%)
<b>Powder 1 (P1)</b>	0.6		
<b>Powder 2 (P2)</b>	0.9		
<b>Powder 3 (P3)</b>	1.0		
<b>Powder 4 (P4)</b>	1.1	400	0.8
<b>Powder 5 (P5)</b>	1.2		
<b>Powder 6 (P6)</b>	1.3		
<b>Powder 7 (P7) - nanoLAMpowder</b>	1.5		

### *Particle size and morphology*

After the particle size determination (Table 11.), the following comments can be made: long milling time causes smaller mean particle size and standard deviation. This can be explained

by the non-aggregated property of the LAM particles due to the milling. P7 sample showed the best values in this case too with a very small average particle size of LAM (97.46 nm). This small particle size, the homogenous distribution and the uniqueness of the LAM particles cause the API to leave the surface of the polymer easier. This property resulted in the best dissolution rate (97.32±4.95% released LAM after 10 mins) among the tested samples. The only sample that did not correspond with the criteria (the target particle size of LAM was 250 nm) was P1, which can be explained by the short milling time. In the SEM picture of the sample, heterogeneous distribution, large-sized particles, and adhesion can be seen, which may lead to good dissolution, but due to these properties and high standard deviation, the reproducibility of the sample and these results are quite uncertain.

**Table 11.** The results of particle size analysis

Sample	Y1- Mean size of LAM (nm)	Y2- Standard Deviation (± nm)
Powder 1 (P1)	521.42	310
Powder 2 (P2)	212.77	150
Powder 3 (P3)	198.71	120
Powder 4 (P4)	143.36	80
Powder 5 (P5)	124.18	60
Powder 6 (P6)	140.62	70
Powder 7 (nanoLAMpowder)	97.46	60

#### *In vitro dissolution test*

The results of the *in vitro* dissolution test can be seen in Table 12. They show that the highest amount of LAM was dissolved from the sample that was prepared according to the robust setpoint. 80.48% of the API dissolved from the sample after 5 min and 97.32% after 10 min, respectively. It means that only this formulation fulfilled the predefined target response values (<85% dissolved LAM after 5 min, 100% dissolved LAM after 10 min). The rest of the formulations performed also well during the test, but except for nanoLAMpowder, just two formulations (P1, P4) responded to the predetermined criteria of this test. An explanation of the unexpected good dissolution results in the case of P1 can be that there are small particles that can leave the polymer matrix easily as well as the aggregated particles can disaggregate easily. However, these mechanisms cannot be controlled, which will lead to uncertain reproducibility as it was mentioned above.

**Table 12.** The result of the *in vitro* dissolution rate study

Sample	Y3- Dissolved amount of LAM after 5 minutes (%)	Y4- Dissolved amount of LAM after 10 minutes (%)
Powder 1 (P1)	71.24	87.47
Powder 2 (P2)	61.06	73.78
Powder 3 (P3)	64.67	73.27
Powder 4 (P4)	77.04	89.52
Powder 5 (P5)	66.20	72.03
Powder 6 (P6)	63.69	76.63
Powder 7 (nanoLAMpowder)	80.48	97.32

#### 5.1.4. *In vivo* studies

The nanoLAMpowder formulation was compared to the PM and IV injection. In the case of IV and intranasal administration, the concentration values of LAM in the blood plasma vs. time profiles are shown in Figure 15. Compared to the nasal formulations, the plasma concentration of LAM was significantly higher in the IV group ( $2.38 \pm 0.14$  mg/L) in the first 3 min which provided the highest measured plasma concentration after the initiation of the injection. There were significant differences between the plasma concentrations in the case of nasal powder forms only in the first 3 min after application, however, these values were negligible compared to the IV administration. This means that there was no considerable difference in the absorption of the API into the systemic circulation by intranasal formulations.

The AUC corresponds to the amount of drug absorbed into the systemic circulation during the investigated period. There were no remarkable differences between the plasma AUC values of powders (PM:  $8.59 \pm 1.35$   $\mu\text{g}/\text{mL} \cdot \text{min}$ ; nano LAM powder:  $13.63 \pm 1.95$   $\mu\text{g}/\text{mL} \cdot \text{min}$ ), however, they were significantly lower than the AUC values of IV administration ( $118.35$   $\mu\text{g}/\text{mL} \cdot \text{min}$ ) (Figure 15.). This could be explained with the 100% bioavailability of the drug after IV application, which can be achieved only in the case of intravascular administration.

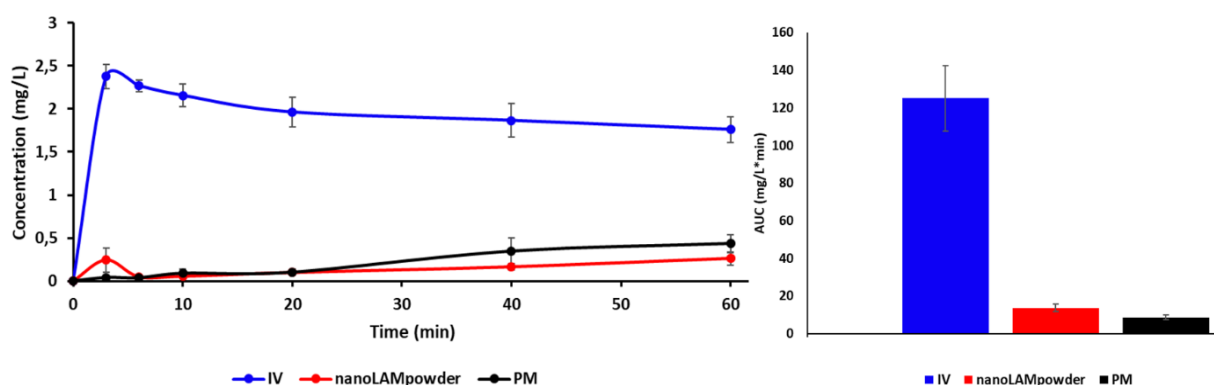


**Figure 15.** The concentration and AUC values of LAM in the blood plasma in case of IV and intranasal administration.

The concentration values of LAM in the brain samples are shown in Figure 16. The application of nanoLAMpowder sample resulted in a significantly higher drug concentration ( $2.16 \pm 0.21$   $\mu\text{g}/\text{brain g}$ ) in brain tissues compared to the PM ( $0.18 \pm 0.76$   $\mu\text{g}/\text{brain g}$ ). The transport of the drug could be assumed by both intranasal formulations, because the drug was presented in the brain 3 min after administration, which period was not enough for the API to pass through the BBB after absorption into the systemic circulation from the nasal mucosa. In the case of PM, the drug-level in the brain was increased 40 min after application, which could be explained by the slower dissolution of microsized LAM particles and with the drug absorption through the BBB from the blood plasma.



In terms of cerebral AUC values of the formulations (Figure 16.), the administration of IV injection resulted in a higher AUC value ( $253.60 \pm 7.66 \mu\text{g}/\text{brain g} \cdot \text{min}$ ) compared to the nasal formulations. This phenomenon could be elucidated with the 100% presence of the drug in the blood plasma after IV application, which may be absorbed through the BBB to target the brain. Due to the quick dissolution of nanoparticles, a higher amount of LAM could reach the brain directly by axonal transport in the case of nanoLAMPowder ( $69.05 \pm 10.08 \mu\text{g}/\text{brain g} \cdot \text{min}$ ), resulting higher AUC values than with the usage of PM ( $54.01 \pm 15.39 \mu\text{g}/\text{brain g} \cdot \text{min}$ ).

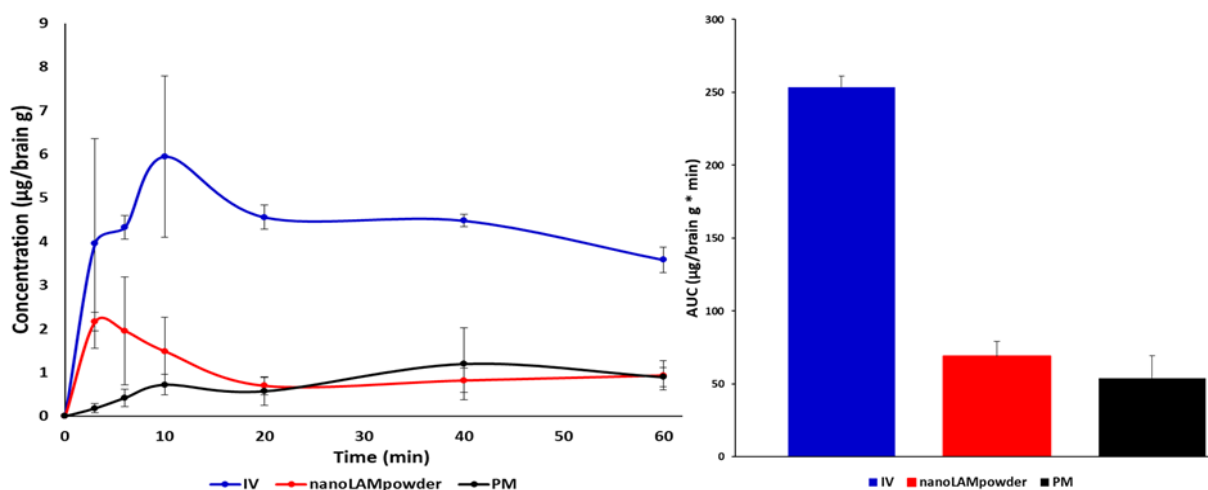


**Figure 16.** The concentration and AUC values of LAM in the brain samples.

To determine the utilization of the drug in the brain tissue, the absolute bioavailability was calculated, where the brain AUC – resulted by IV injection – was considered as 100% (Table 13.). In the case of nanoLAMPowder, the absolute bioavailability of LAM was 39.84%, while in the case of PM it was only approximately 21%.

The cerebral drug targeting efficiency index (DTE) reflects the relative accumulation of the drug in the brain following intranasal administration as compared to systemic administration. DTE data were above 1.0 in case of both nasal powders, as the LAM could reach the brain tissues more efficiently via axonal transport, than through the systemic circulation. This resulted in remarkable absorption through the nasal mucosa directly into the CNS and parallelly resulted in poor transepithelial absorption into the systemic circulation.

**Table 13.** Calculated parameters of intranasal powders applying IV administration as a benchmark.

	abs. BA for the brain (%)	AUC <sub>brain</sub> /AUC <sub>blood</sub>	DTE
IV injection	100	2.02	1
nano LAM powder	39.84	5.06	2.49
PM	21.30	6.29	3.11

### 5.1.5. Stability study of the nanoLAMPowder

In the tested period, the key properties related to the powder formulation did not change considerably. The results of particle size determination resulted in same particle size of the product during the examined period (Table 14.), which shows that the product's particles did



not aggregate. The size falls into the range which is desired in the case of nasal powders, which is 10-40  $\mu\text{m}$ .

**Table 14.** The results of particle size investigation the product. In the table n.s means that there is no significant difference at 95% level.

	Average size of the product ( $\mu\text{m}$ )	t-value	p-value	Significance
<b>1-day</b>	29.91 $\pm$ 15.85	-0.1435	0.8883	n.s.
<b>3 months</b>	28.48 $\pm$ 12.81	0.2994	0.7690	n.s.
<b>6 months</b>	26.52 $\pm$ 11.14	0.9064	0.3801	n.s.

The particle size of LAM in the formulation showed an increase with relatively high standard deviation (Table 15.). However, according to results of the statistical analysis there is no significant difference in the particle sizes during the storage period, thus the previously experienced rapid and high degree of release was predicted.

**Table 15.** The results of particle size investigation of LAM. In the table n.s means that there is no significant difference at 95% level.

	Average size of LAM (nm)	t-value	p-value	Significance
<b>1-day</b>	97 $\pm$ 60	1.2382	0.2347	n.s.
<b>3 months</b>	105 $\pm$ 77	0.7934	0.4408	n.s.
<b>6 months</b>	120 $\pm$ 84	-0.0408	0.9687	n.s.

The results of the structural investigations (DSC and XRPD) confirmed that the LAM remained partly amorphous in the tested period. Moreover, according to the results of *in vitro* dissolution tests the rapid release of LAM was maintained during the examined period.

## 5.2. Development of NC formulations

### 5.2.1. Identification of factors affecting product quality

The first step before the experiment was to identify and systematize the most influencing factors that could affect product quality. This scheme allowed us to design our research plan more effectively, optimizing costs and time. In the Ishikawa-diagram of the NC product, we could identify 4 main groups of influencing factors (Figure 17.): material characteristics, production method, investigation methods and, therapeutical and regulatory expectations. Among these factors, the type and amount of surfactant, liquid lipid, surface modifier, coating material and cryoprotectant, the amount of API and the particle size, its PDI and the surface characteristics (ZP) of the NCs have the greatest impact on the quality of the product. The rest of the factors were not found to be as influencing during the preformulation tests and the literature review. After setting up the Ishikawa-diagram we decided to set up a factorial experimental plan, where the type of the coating material and the liquid lipid was varied. The experiments were optimized for particle size and PDI.

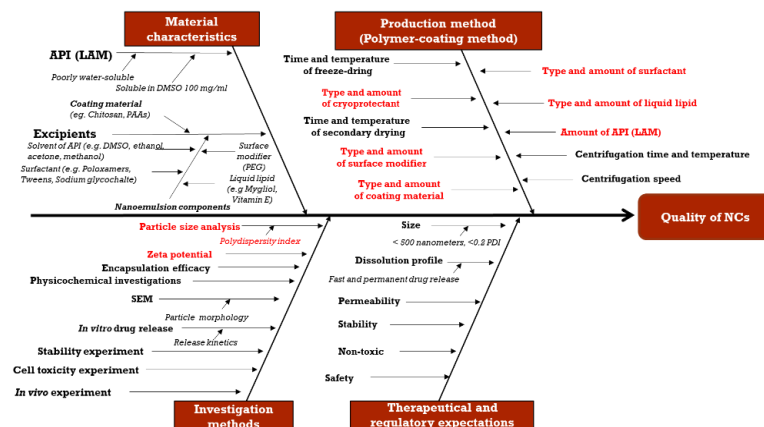


**Figure 17.** Ishikawa-diagram of the NC product

### 5.2.2. Particle size, particle size distribution and surface charge characterization of NCs

As a first step, the particle size and surface charge of the NCs were analyzed (Table 16.). The NCs were always in the 290-380 nm range that is acceptable according to the FDA regulatory, as the particle size of nanosystems has to be between 100-1000 nm [107]. Our aim was to develop NCs that were in the lower part of this range and showed a homogenous particle size population (PDI <0.2). These requirements were fulfilled for the NCs only if the liquid lipid:surfactant ratio was 1:1. LAM incorporation resulted in a significant increase in particle size as compared to blank NCs. In all cases, zeta potential values were similar, positive and close to zero that may be advantageous for mucoadhesion and mucodiffusion [108]. In the other samples, the particle size and PDI did not meet the criteria that we had set previously, and the particles were not in the nano range, so in the following the most promising sample was tested. The freeze-dried formulation showed some increase in particle size and PDI after redispersion ( $504 \pm 3$  nm, 0.538 PDI), indicating some aggregation, that could happen due to the presence of mannitol. However, this aggregation was not observed on the freeze-dried state when the powder cake was analyzed with imaging technology as the particle size showed  $179 \pm 62$  nm. This means that the NCs maintained their size after freeze-drying. Another relevant observation was an increase in zeta potential in the NCs resuspended after freeze-drying, which can be explained by the presence of the cryoprotectant. The  $26.5 \pm 0.9$  value means that the NCs may have high degrees of stability.

**Table 16.** Results of the particle size and surface characterization of the NCs.

	Z-average (d. nm)	PDI	Zeta potential (mV)
<b>Blank NCs after centrifugation (2:1 ratio)</b>	$2815 \pm 159$	0.795	$0.99 \pm 0.4$
<b>LAM NCs after centrifugation (2:1 ratio)</b>	$1210 \pm 68$	0.773	$1.3 \pm 0.1$
<b>Blank NCs after centrifugation (1:2 ratio)</b>	$1477 \pm 72$	0.643	$0.80 \pm 0.3$
<b>LAM NCs after centrifugation (1:2 ratio)</b>	$1399 \pm 59$	0.950	$0.94 \pm 0.5$
<b>Blank NCs after centrifugation (1:1 ratio)</b>	$294 \pm 9$	0.175	$0.39 \pm 0.2$
<b>LAM NCs after centrifugation (1:1 ratio)</b>	$305 \pm 7$	0.188	$1.0 \pm 0.3$
<b>FDNCs</b>	Freeze-dried: $179 \pm 62$ After redispersion: $504 \pm 3$	0.538	$26.5 \pm 0.9$

### 5.2.3. Encapsulation efficacy (EE) and drug loading (DL)

The EE of LAM was  $58.44\% \pm 4.81$  in the NCs and the DL was  $5.31\% \pm 0.67$ . This is an acceptable level of EE for a nanoformulation, particularly since it was achieved with a very high drug loading.

### 5.2.4. Particle morphology

We analyzed LAM-loaded FDNCs (Figure 18. A) and freeze-dried NCs (Figure 18. B) by SEM. The core and shell substructures of the NCs were clearly visible before freeze-drying. In both cases, NCs presented a spherical shape and homogenous distribution. There was no sign of non-encapsulated, crystalline LAM around the NCs and there was no sign of aggregation in the mannitol matrix, so the pictures indicated good particle stability and no warnings regarding drug aggregation.

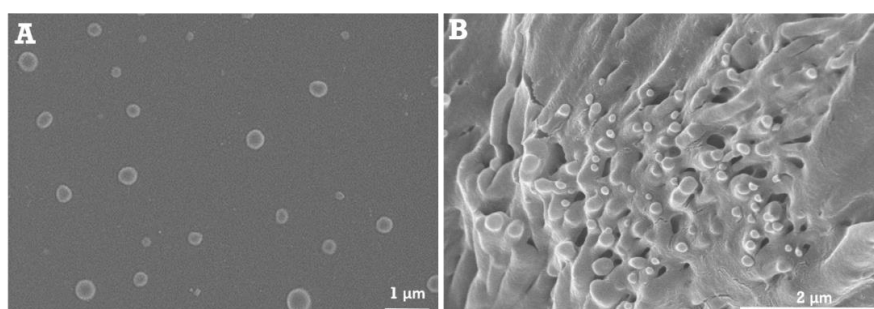


**Figure 18.** The morphology of LAM loaded NCs (Picture A.) and FDNCs (Picture B.)

### 5.2.5. *In vitro* drug release and permeability studies

The *in vitro* release study showed faster release of LAM in the case of both NCs formulations compared to pure LAM powder (Figure 19. A). It was detected that more than 20% of LAM released after 5 min and ~60 % LAM after 15 min; afterward, a drug release plateau was observed. The FDNCs released the drug slower than NCs but markedly faster than the drug powder. In this case, ~40% LAM was released after 10 min, and 50% after 15 min, a point where the release started to level-off. At 15 min, both NCs formulations released between 2.5 and 3-fold more LAM than the drug powder. For nasal administration, the first four points are the most important, because the mucociliary clearance renews the nasal mucus approximately every 15 min, thus limiting the API residence time at this site. In this sense, the fast release of LAM from the nanoformulations can be considered an advantageous characteristic for nasal delivery. Moreover, the use of chitosan may extend the residence time, which means that the formulation could have enough time to get into the CNS.

Next, we performed a permeability study to compare how the different formulations could modify the capacity of LAM for crossing biological barriers (Figure 19. B). In the case of nasal administration, it is important to achieve a high permeability rate through the mucosa, which means that the API reaches its target more efficiently. NCs and FDNCs formulations performed similarly well in this experiment, and much better than a LAM powder, which achieved the lowest amount of permeated drug. In the case of the NCs formulations,

~25  $\mu\text{g}/\text{cm}^2$  LAM diffused through the membrane, which is 2.5 times higher than the amount of drug diffused from the raw powder formulation. This was a remarkably high amount if we take into consideration that an average human nasal mucosa is around 150-200  $\text{cm}^2$  [26].

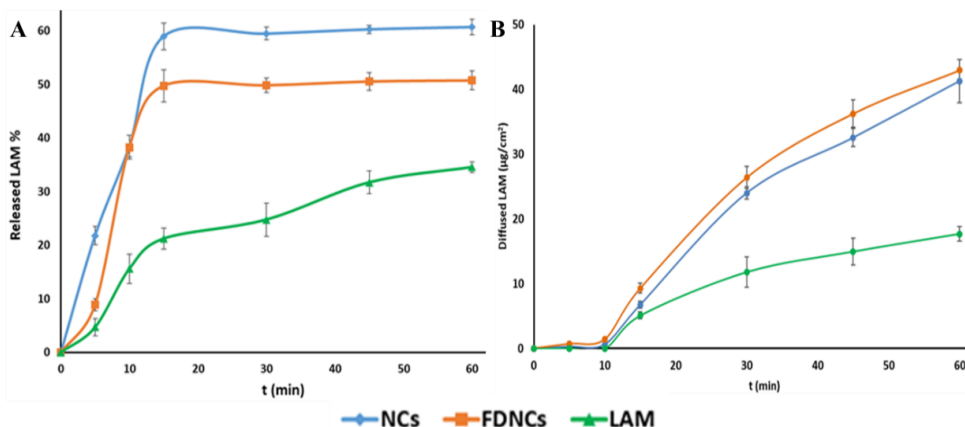


**Figure 19.** *In vitro* drug release (A) and permeability (B) studies of different NCs formulations and LAM powder

The calculated Flux (J) and permeability coefficient ( $K_p$ ) values (Table 17.). The Flux shows how much API can diffuse through the membrane per hour and the surface unit, while  $K_p$  is the Flux-donor phase ratio. The results of the table show that the LAM could diffuse in higher amounts through the membrane to the acceptor phase from the NC formulations than from the powder and that there was no significant difference between both nanoformulations. These results validated the previous observations on drug diffusion, as the NC formulations showed higher values for these parameters than the powder.

**Table 17.** Calculated Flux (J) and permeability coefficient ( $K_p$ ) values for the different LAM formulations

	J ( $\mu\text{g}/\text{cm}^2/\text{h}$ )	$K_p$ (cm/h)
LAM	31.48	0.021
NCs	41.29	0.023
FDNCs	42.96	0.03

### 5.2.6. *In vivo* drug release study

In a final step, we performed the *in vivo* administration of the LAM formulations and we performed PK analysis both in the blood and brain (Figure 20. and 21., respectively). The plasma concentration of LAM was significantly higher for the NCs group than for the FDNCs group, and this was particularly remarkable in the 3 min datapoint:  $0.18 \pm 0.03 \mu\text{g}/\text{mL}$  vs.  $0.01 \pm 0.002 \mu\text{g}/\text{mL}$  LAM concentration for NCs and FDNCs, respectively. This could be explained by the fact that the API reached the systemic circulation without passing through the liver. Another possible explanation of the relatively high absorption of liquid NCs is that the liquid could spread over a larger surface that caused higher plasma concentrations. Moreover, another possible explanation of the poor permeation of the FDNCs is that in the nasal cavity the amount of water is limited. As the solid particles need to be solubilized before permeation, this limited amount of water can retard or even limit the extent of the absorption.

The ratio of AUC values shows that the API from the liquid NCs reached the plasma 12.28-fold more than the API in freeze-dried NCs ( $AUC_{(NCs)}=6.13 \pm 0.52 \text{ min} \cdot \mu\text{g/mL plasma}$ ;  $AUC_{(FDNCs)}= 0.50 \pm 0.16 \text{ min} \cdot \mu\text{g/mL}$ ), but they were well below the IV formulation ( $125.08 \pm 17.46 \text{ min} \cdot \mu\text{g/mL}$ ).

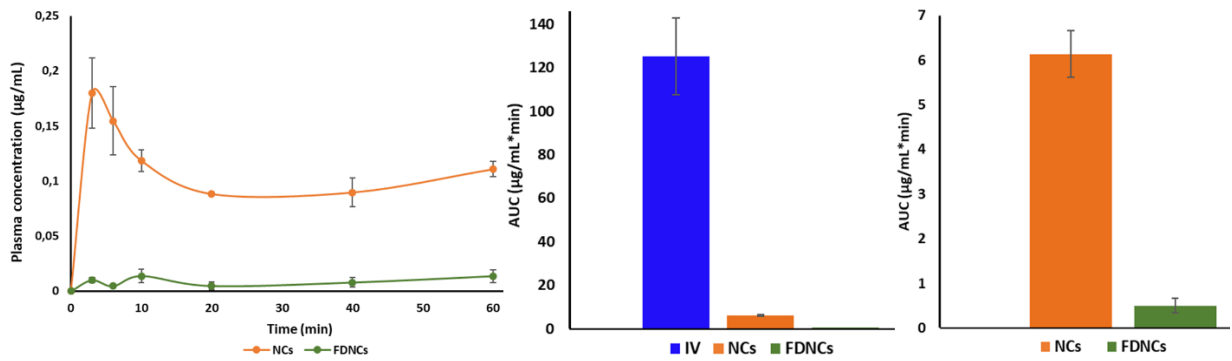


**Figure 20.** The concentration values and AUC of LAM in the blood plasma.

Nasal administration of LAM in NCs achieved higher brain drug concentrations than FDNCs. Indeed, NCs resulted in significantly higher AUC values ( $11.65 \pm 1.03 \text{ min} \cdot \mu\text{g/g}$ ) than FDNCs ( $2.06 \pm 1.10 \text{ min} \cdot \mu\text{g/g}$ ), while the AUC value of IV administration was  $250.603 \pm 7.66 \text{ min} \cdot \mu\text{g/brain g}$ . The ratio of AUC values between the liquid and the solid NCs was 5.65, which means that this formulation could provide better drug absorption. In any case, LAM was present in the CNS shortly after administration since it was detected there even at the 3 min extraction point. This time seems too short for LAM to be absorbed and to cross through the BBB, which indicates a possible axonal transport of the drug. Besides, in the case of FDNCs, the drug would take more time to be absorbed into the systemic circulation (Figure 21.) through the nasal mucosa, but it is still detected in the CNS. FDNCs showed very constant LAM levels in the CNS after the first 10 min, and we hypothesize that this could be due to the presence of parallel transport mechanism of axonal transport and access through the BBB.

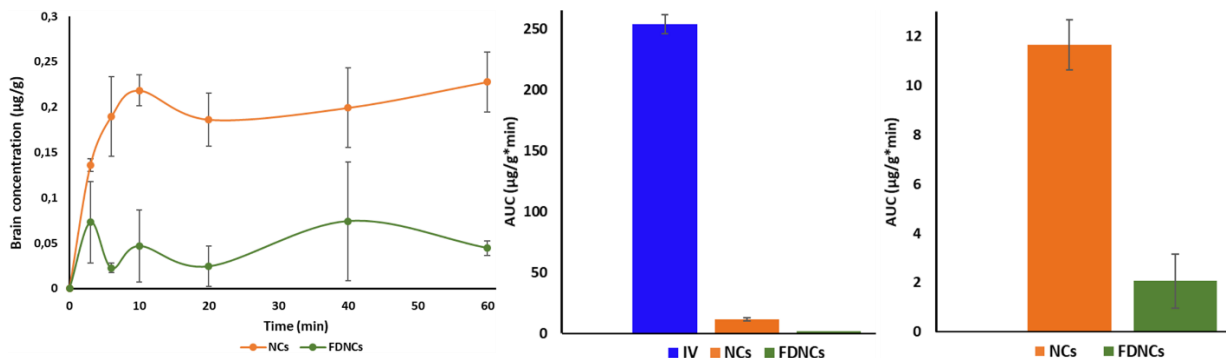


**Figure 21.** The concentration and AUC values of LAM in the brain samples.

Table 18. represents the calculated values of the investigation. The brain: plasma ratios of the NCs and FDNCs were 1.90, and 4.13, respectively. This means that the API was more concentrated in the CNS than in blood plasma. The fact that this value is higher for the FDNCs than for the NCs indicates that this concentration ratio is not only dependent on drug

biodistribution, but rather on other biopharmaceutical processes. We think that this higher ratio achieved with FDNCs could indicate a higher contribution of direct axonal drug transport for this formulation as compared to NCs.

The cerebral drug targeting efficiency index (DTE) reflects the relative accumulation of the drug in the brain following intranasal administration as compared to systemic administration. DTE data was around 1.0 in the case of NCs, which means that LAM presented in similar concentrations in plasma and brain tissues, respectively. As for the FDNCs, the LAM could reach the brain tissues two times more efficiently via axonal transport, than through the systemic circulation, which is indicated by the value above 2.0. This resulted in remarkable absorption through the nasal mucosa directly into the CNS and parallelly resulted in poor transepithelial absorption into the systemic circulation in case of the solid-state sample.

**Table 18.** Calculated parameters of intranasal powders applying IV administration as a benchmark.

	$AUC_{\text{brain}}/AUC_{\text{blood}}$	DTE
<b>IV injection</b>	2.02	1
<b>NCs</b>	1.90	0.94
<b>FDNCs</b>	4.13	2.04

### 5.3. Comparison of NP and NC formulations based on their *in vivo* performance

Table 19. summarizes the main *in vivo* properties of the samples. It can be seen that the nanoLAM powder had the greatest presence in the brain tissues and also in the plasma. Generally, compared to the NP samples, the NC formulations showed smaller AUC values. Moreover, the targeting of LAM into the CNS was much better in the case of NPs which can be seen from  $AUC_{\text{brain}}/AUC_{\text{blood}}$  data. The DTE values of NPs were also higher compared to the NCs, which means that LAM could reach its site of effect more efficiently when administered in powder formulation. The differences can be explained by the administered dose which is much higher in the case of NPs because the drug loading capacity of NCs is limited. Accordingly, the application of NP formulations can be advantageous because of the higher dose that can be administered into the nostril.

**Table 19.** Calculated parameters of the formulations.

	$AUC_{\text{brain}} (\text{min} \cdot \mu\text{g}/\text{g})$	$AUC_{\text{blood}} (\text{min} \cdot \mu\text{g}/\text{mL})$	$AUC_{\text{brain}}/AUC_{\text{blood}}$	DTE
<b>PM</b>	54.01±15.39	8.59±1.35	6.29	3.11
<b>nanoLAM powder</b>	69.05±10.08	13.63±1.95	5.06	2.49
<b>NCs</b>	11.65±1.02	6.13±0.52	1.90	0.94
<b>FDNCs</b>	2.06±1.10	0.50±0.16	4.13	2.04

## 6. CONCLUSION

### **To summarize the thesis, the following statements can be made according to the aims:**

**I.** After the literature review, it was found that the combination of nasal drug delivery, nanosystems and QbD methodology can be advantageous to develop innovative and improved bioavailability products for LAM. The development of alternative dosage forms for LAM is important because it was found in the literature that on the market, only tablets, disintegrating tablets, and chewable tablets can be found, which can be ineffective in some cases, such as in malabsorption or acute diarrhea. It was also found that there is great potential –despite the poor number of marketed products- in the research and development of NPs, because they have many advantageous properties compared to liquid formulations. Moreover, the development of NCs can eliminate some possible drawbacks of nasal delivery according to the current information found in the literature.

**II.** The quality influencing factors were collected with the help of an Ishikawa diagram. The results of the RA showed that amongst the CQAs, the particle size, its distribution and the dissolution rate of LAM, while amongst the CPPs the LAM:additive ratio, the milling time and speed are the most critical factors of NP production. After the preliminary studies, based on the results of the particle size analysis, *in vitro* release and permeability tests, PVA was chosen to serve as a matrix for nanosized LAM particles. The optimization of the dry milling process was executed with DoE, which meant the Design Space determination and validation of the powder production. Due to the DS estimation, a more economical – time- and material-effective – sample preparation method was set up and the results of nanoLAMpowder (milling time: 1.5 h, milling speed: 400 rpm, PVA:LAM ratio: 0.8) were in the aimed ranges. The results of the *in vitro* dissolution test showed the highest amount of released LAM from nanoLAMpowder during the validation process.

**III.** NanoLAMpowder was tested in further investigations and was compared to its PM. The micrometric investigations showed that the LAM was in the nano range ( $97 \pm 60$  nm) in the case of nanoLAMpowder, while it was aggregated in the PM sample. The results of the *in vitro* dissolution and permeability tests showed a rapid and high release from the nanoLAMpowder. The *in vivo* investigation showed that the plasma concentration of LAM was significantly higher in the IV group during the test compared to the nasally administered samples, among which there was no considerable difference. However, the application of nano LAM containing sample resulted in a significantly higher drug concentration in the brain tissues compared to the PM. Also, the presence of LAM in the CNS was higher in the case of nanoLAMpowder according to the AUC values. The axonal transport of the drug was assumable by both intranasal formulations. The results of the stability studies showed that the key properties (particle size, crystallinity properties, *in vitro* release profile) of the NP did not

change significantly, so the efficiency presumably maintained during the tested period. According to our aims, we were able to develop an inline, modified diffusion method, which is a more accurate, easy-to-implement, more informative method that has made our measurements more simple and more efficient.

**IV.** Then, the aim was to develop and investigate novel, LAM containing core-shell NCs. The identification and prioritization of most influencing factors were collected with the help of an Ishikawa diagram. The components of the NC formulation were determined. According to the results of the preliminary experiments and size optimization, chitosan-coated NCs with LAM were formulated both as a liquid suspension and as a freeze-dried powder.

**V.** The following step was the optimization of the main influencing factors of production. Accordingly, the parameters of freeze-drying were set and the most promising cryoprotectant (mannitol) was determined. Then, during the investigation procedure, the particle size of LAM NCs was under 500 nm, the zeta potential was nearly neutral in the case of NCs, while they turned out to be positive in the case of FDNCs. LAM released quickly from both NC formulations, with 50% payload released after 15 min. The permeation rate of LAM was also higher for the NC samples than for LAM in powder form. *In vivo* studies showed that LAM could reach the brain in significant amounts, particularly in the case of NCs. The kinetics and biodistribution ratio of the drug between brain and plasma suggest that there is axonal transport involved in drug absorption, which means that the LAM can reach its site of action in an amount sufficient for effect.

**VI.** In the living body, nanosystems could be more effective due to the fact that their smaller particle size leads to a larger specific surface, which usually results in higher dissolution rate and increased adhesion to mucous membranes. Powder formulations, when administered through the nose, can withdraw water. This could be advantageous because the tight junctions are widened thanks to which the API can pass easier through the membrane and, at the same time, the formulation becomes a bit viscous, which may increase its residence time on the mucosa. In the case of nanoLAM powder, PVA was used as a mucoadhesive, wetting agent, which provided a great matrix for LAM nanoparticles. Due to the presence of PVA, the co-milling was more effective, and the small particles could leave the water-soluble matrix easily, which resulted in a great *in vitro* and *in vivo* performance. As for the NCs, chitosan was served as a shell component for the nanoparticles. This coating material can extend the residence time on the nasal mucosa and can improve the adhesion to the mucosa, which resulted in great API presence in the CNS in our case. However, according to the *in vivo* results of the NP and NC formulations, it can be concluded that the presence of LAM in CNS was significantly higher in the case of NPs and also, the targeting of LAM was better. In the case of NCs, it is not possible to encapsulate large amounts of API into the capsules, which



results in lower administration doses. As for NPs, the administration dose is much higher, which in our case, resulted in better in vivo performance. Therefore, and because of the much more simple, economical and ecological sample production method, in our opinion, the NPs could provide a great, short-term alternative for the marketed tablets in the therapy of epilepsy, if their application is not possible.

### **New findings of the work:**

✓ As there is a limited number of nasal powder products on the market, the availability of information about them is poor despite, there is a great potential in their application. Their stability is better, the administration dose is higher compared to the liquid formulation, the residence time on mucosal surfaces is longer, fewer additives are needed during the formulation process. Also, these systems are special because their design, development, and optimization should be parallel with those of the delivery device to assure proper dosing. Thus, the thesis provides up-to-date and summarized knowledge about NPs.

✓ The determination of QTPP of nasal powder products and the collection of the most influencing CQAs (particle size, particle distribution and dissolution rate of LAM) and CPPs (milling time, milling speed, API: additive ratio). The dry milling sample production method was validated. Accordingly, a novel, partially amorphous, nanosized LAM containing, brain targeted NP was developed, which could provide an alternative for tablets when their administration is not possible. The formulation is necessary because there are no other LAM containing dosage forms on the market, just tablets. The LAM could release from the formulation rapidly and in a high amount.

✓ Adaptation, development and validation of a permeability investigation method. The modified diffusion model is suitable for inline, real-time detection, adapted to nasal conditions, using small volumes of phases, appropriately impregnated membrane, to monitor the diffusion of the drug, and to determine its concentration in the acceptor and donor phases. Accordingly, we have succeeded in developing an easy-to-implement, easy-to-reproduce, accurate, informative and time-efficient method.

✓ The development of a LAM containing, nanostructured NC formulation for nasal administration. Optimized technological protocol to prepare an intermediate sample containing NC. The formulation can be administered in liquid and solid forms. The NC formulation can offer a great alternative for LAM administration into the CNS in a considerably high amount. Using this kind of nanoformulation, the advantages of nanosystems and nasal delivery can be combined.

✓ The developed formulations can be suitable-especially the NP formulation- for application in the therapy of epilepsy for a short time instead of tablets, for example in GI malabsorption or acute diarrhea, after further investigations.

## REFERENCES

- [1] C. Bartos, R. Ambrus, P. Sipos, M. Budai-Szűcs, E. Csányi, R. Gáspár, Á. Márki, A.B. Seres, A. Sztojkov-Ivanov, T. Horváth, P. Szabó-Révész, Study of sodium hyaluronate-based intranasal formulations containing micro- or nanosized meloxicam particles, *International Journal of Pharmaceutics*. 491 (2015) 198–207. <https://doi.org/10.1016/j.ijpharm.2015.06.046>.
- [2] S. Horvát, A. Fehér, H. Wolburg, P. Sipos, S. Veszeka, A. Tóth, L. Kis, A. Kurunczi, G. Balogh, L. Kürti, I. Erős, P. Szabó-Révész, M.A. Deli, Sodium hyaluronate as a mucoadhesive component in nasal formulation enhances delivery of molecules to brain tissue, *European Journal of Pharmaceutics and Biopharmaceutics*. 72 (2009) 252–259. <https://doi.org/10.1016/j.ejpb.2008.10.009>.
- [3] H. Kublik, M.T. Vidgren, Nasal delivery systems and their effect on deposition and absorption, *Advanced Drug Delivery Reviews*. 29 (1998) 157–177. [https://doi.org/10.1016/S0169-409X\(97\)00067-7](https://doi.org/10.1016/S0169-409X(97)00067-7).
- [4] L. Nasare, K. Niranjane, A. Nagdevte, S. Mohril, NASAL DRUG DELIVERY SYSTEM: AN EMERGING APPROACH FOR BRAIN TARGETING, *World Journal of Pharmacy and Pharmaceutical Sciences*. 3 (n.d.) 15.
- [5] A. Mistry, S. Stolnik, L. Illum, Nanoparticles for direct nose-to-brain delivery of drugs, *International Journal of Pharmaceutics*. 379 (2009) 146–157. <https://doi.org/10.1016/j.ijpharm.2009.06.019>.
- [6] E. Prommer, L. Thompson, Intranasal fentanyl for pain control: current status with a focus on patient considerations, *Patient Preference and Adherence*. (2011) 157. <https://doi.org/10.2147/PPA.S7665>.
- [7] D.M. Vasa, I.S. Buckner, J.E. Cavanaugh, P.L.D. Wildfong, Improved Flux of Levodopa via Direct Deposition of Solid Microparticles on Nasal Tissue, *AAPS PharmSciTech*. 18 (2017) 904–912. <https://doi.org/10.1208/s12249-016-0581-4>.
- [8] R. Narayan, M. Singh, O. Ranjan, Y. Nayak, S. Garg, G.V. Shavi, U.Y. Nayak, Development of risperidone liposomes for brain targeting through intranasal route, *Life Sciences*. 163 (2016) 38–45. <https://doi.org/10.1016/j.lfs.2016.08.033>.
- [9] R.L. Shinde, G.P. Bharkad, P.V. Devarajan, Intranasal microemulsion for targeted nose to brain delivery in neurocysticercosis: Role of docosahexaenoic acid, *European Journal of Pharmaceutics and Biopharmaceutics*. 96 (2015) 363–379. <https://doi.org/10.1016/j.ejpb.2015.08.008>.
- [10] Z.N. Warnken, H.D.C. Smyth, A.B. Watts, S. Weitman, J.G. Kuhn, R.O. Williams, Formulation and device design to increase nose to brain drug delivery, *Journal of Drug Delivery Science and Technology*. 35 (2016) 213–222. <https://doi.org/10.1016/j.jddst.2016.05.003>.
- [11] C. Bartos, R. Ambrus, A. Kovács, R. Gáspár, A. Sztojkov-Ivanov, Á. Márki, T. Janáky, F. Tömösi, G. Kecskeméti, P. Szabó-Révész, Investigation of Absorption Routes of Meloxicam and Its Salt Form from Intranasal Delivery Systems, *Molecules*. 23 (2018) 784. <https://doi.org/10.3390/molecules23040784>.
- [12] M. Agrawal, S. Saraf, S. Saraf, S.G. Antimisiaris, M.B. Chougule, S.A. Shoyele, A. Alexander, Nose-to-brain drug delivery: An update on clinical challenges and progress towards approval of anti-Alzheimer drugs, *Journal of Controlled Release*. 281 (2018) 139–177. <https://doi.org/10.1016/j.jconrel.2018.05.011>.
- [13] R.P. Chen, From Nose to Brain: The Promise of Peptide Therapy for Alzheimer’s Disease and Other Neurodegenerative Diseases, *Journal of Alzheimer’s Disease & Parkinsonism*. 07 (2017). <https://doi.org/10.4172/2161-0460.1000314>.
- [14] X. Yan, L. Xu, C. Bi, D. Duan, L. Chu, X. Yu, Z. Wu, A. Wang, K. Sun, Lactoferrin-modified rotigotine nanoparticles for enhanced nose-to-brain delivery: LESA-MS/MS-based drug biodistribution, pharmacodynamics, and neuroprotective effects, *International Journal of Nanomedicine*. Volume 13 (2018) 273–281. <https://doi.org/10.2147/IJN.S151475>.
- [15] M.R. Patel, R.B. Patel, K.K. Bhatt, B.G. Patel, R.V. Gaikwad, Paliperidone microemulsion for nose-to-brain targeted drug delivery system: pharmacodynamic and pharmacokinetic evaluation, *Drug Delivery*. 23 (2016) 346–354. <https://doi.org/10.3109/10717544.2014.914602>.
- [16] F. Erdő, L.A. Bors, D. Farkas, Á. Bajza, S. Gizurarson, Evaluation of intranasal delivery route of drug administration for brain targeting, *Brain Research Bulletin*. 143 (2018) 155–170. <https://doi.org/10.1016/j.brainresbull.2018.10.009>.
- [17] E. Gavini, G. Rassu, L. Ferraro, S. Beggiato, A. Alhalaweh, S. Velaga, N. Marchetti, P. Bandiera, P. Giunchedi, A. Dalpiaz, Influence of polymeric microcarriers on the in vivo

- intranasal uptake of an anti-migraine drug for brain targeting, *European Journal of Pharmaceutics and Biopharmaceutics*. 83 (2013) 174–183. <https://doi.org/10.1016/j.ejpb.2012.10.010>.
- [18] T. Horváth, R. Ambrus, G. Völgyi, M. Budai-Szűcs, Á. Márki, P. Sipos, C. Bartos, A.B. Seres, A. Sztojkov-Ivanov, K. Takács-Novák, E. Csányi, R. Gáspár, P. Szabó-Révész, Effect of solubility enhancement on nasal absorption of meloxicam, *European Journal of Pharmaceutical Sciences*. 95 (2016) 96–102. <https://doi.org/10.1016/j.ejps.2016.05.031>.
- [19] F. Rinaldi, L. Seguella, S. Gigli, P.N. Hanieh, E. Del Favero, L. Cantù, M. Pesce, G. Sarnelli, C. Marianecchi, G. Esposito, M. Carafa, inPentosomes: An innovative nose-to-brain pentamidine delivery blunts MPTP parkinsonism in mice, *Journal of Controlled Release*. 294 (2019) 17–26. <https://doi.org/10.1016/j.jconrel.2018.12.007>.
- [20] E. Gavini, A. Hegge, G. Rassu, V. Sanna, C. Testa, G. Pirisino, J. Karlsen, P. Giunchedi, Nasal administration of Carbamazepine using chitosan microspheres: In vitro/in vivo studies, *International Journal of Pharmaceutics*. 307 (2006) 9–15. <https://doi.org/10.1016/j.ijpharm.2005.09.013>.
- [21] L. Tiozzo Fasiolo, M.D. Manniello, E. Tratta, F. Buttini, A. Rossi, F. Sonvico, F. Bortolotti, P. Russo, G. Colombo, Opportunity and challenges of nasal powders: Drug formulation and delivery, *European Journal of Pharmaceutical Sciences*. 113 (2018) 2–17. <https://doi.org/10.1016/j.ejps.2017.09.027>.
- [22] Magyarországon forgalomba hozott nazális készítmények, (2020). <https://www.ogyei.gov.hu/nyitoidal>.
- [23] R.P. Chen, From Nose to Brain: The Promise of Peptide Therapy for Alzheimer’s Disease and Other Neurodegenerative Diseases, *Journal of Alzheimer’s Disease & Parkinsonism*. 07 (2017). <https://doi.org/10.4172/2161-0460.1000314>.
- [24] N. Sharma, N. Mishra, IMPORTANCE OF LIPID NANOPARTICLES IN THE TREATMENT OF EPILEPSY: A FOCUS ON NASAL DELIVERY, *Journal of Pharmaceutical & Scientific Innovation*. 3 (2014) 199–207. <https://doi.org/10.7897/2277-4572.033140>.
- [25] G.D. Anderson, R.P. Saneto, Current oral and non-oral routes of antiepileptic drug delivery, *Advanced Drug Delivery Reviews*. 64 (2012) 911–918. <https://doi.org/10.1016/j.addr.2012.01.017>.
- [26] M. Kapoor, J.C. Cloyd, R.A. Siegel, A review of intranasal formulations for the treatment of seizure emergencies, *Journal of Controlled Release*. 237 (2016) 147–159. <https://doi.org/10.1016/j.jconrel.2016.07.001>.
- [27] P.K. Gangurde, N. Ajitkumar B., L. Kumar, Lamotrigine Lipid Nanoparticles for Effective Treatment of Epilepsy: a Focus on Brain Targeting via Nasal Route, *Journal of Pharmaceutical Innovation*. 14 (2019) 91–111. <https://doi.org/10.1007/s12247-018-9343-z>.
- [28] D.P. Wermeling, Intranasal delivery of antiepileptic medications for treatment of seizures, *Neurotherapeutics*. 6 (2009) 352–358. <https://doi.org/10.1016/j.nurt.2009.01.002>.
- [29] M. Pozzoli, P. Rogueda, B. Zhu, T. Smith, P.M. Young, D. Traini, F. Sonvico, Dry powder nasal drug delivery: challenges, opportunities and a study of the commercial Teijin Puvlizer Rhinocort device and formulation, *Drug Development and Industrial Pharmacy*. 42 (2016) 1660–1668. <https://doi.org/10.3109/03639045.2016.1160110>.
- [30] Z.T. Al-Salama, L.J. Scott, Sumatriptan Nasal Powder: A Review in Acute Treatment of Migraine, *Drugs*. 76 (2016) 1477–1484. <https://doi.org/10.1007/s40265-016-0641-9>.
- [31] Glucagon Nasal Powder (Baqsimi) for Severe Hypoglycemia, (n.d.). [https://secure.medicalletter.org/article-share?a=1581b&p=tml&title=Glucagon%20Nasal%20Powder%20\(Baqsimi\)%20for%20Severe%20Hypoglycemia&cannotaccesstitle=1](https://secure.medicalletter.org/article-share?a=1581b&p=tml&title=Glucagon%20Nasal%20Powder%20(Baqsimi)%20for%20Severe%20Hypoglycemia&cannotaccesstitle=1).
- [32] R. Scherließ, M. Mönckedieck, K. Young, S. Trows, S. Buske, S. Hook, First in vivo evaluation of particulate nasal dry powder vaccine formulations containing ovalbumin in mice, *International Journal of Pharmaceutics*. 479 (2015) 408–415. <https://doi.org/10.1016/j.ijpharm.2015.01.015>.
- [33] T. Parumasivam, R.Y.K. Chang, S. Abdelghany, T.T. Ye, W.J. Britton, H.-K. Chan, Dry powder inhalable formulations for anti-tubercular therapy, *Advanced Drug Delivery Reviews*. 102 (2016) 83–101. <https://doi.org/10.1016/j.addr.2016.05.011>.
- [34] M. Karashima, N. Sano, S. Yamamoto, Y. Arai, K. Yamamoto, N. Amano, Y. Ikeda, Enhanced pulmonary absorption of poorly soluble itraconazole by micronized cocrystal dry powder formulations, *European Journal of Pharmaceutics and Biopharmaceutics*. 115 (2017) 65–72. <https://doi.org/10.1016/j.ejpb.2017.02.013>.

- [35] A. Tanaka, T. Furubayashi, M. Tomisaki, M. Kawakami, S. Kimura, D. Inoue, K. Kusamori, H. Katsumi, T. Sakane, A. Yamamoto, Nasal drug absorption from powder formulations: The effect of three types of hydroxypropyl cellulose (HPC), *European Journal of Pharmaceutical Sciences*. 96 (2017) 284–289. <https://doi.org/10.1016/j.ejps.2016.09.028>.
- [36] L. Tiozzo Fasiolo, M.D. Manniello, E. Tratta, F. Buttini, A. Rossi, F. Sonvico, F. Bortolotti, P. Russo, G. Colombo, Opportunity and challenges of nasal powders: Drug formulation and delivery, *European Journal of Pharmaceutical Sciences*. 113 (2018) 2–17. <https://doi.org/10.1016/j.ejps.2017.09.027>.
- [37] S. Trows, R. Scherließ, Carrier-based dry powder formulation for nasal delivery of vaccines utilizing BSA as model drug, *Powder Technology*. 292 (2016) 223–231. <https://doi.org/10.1016/j.powtec.2016.01.042>.
- [38] C. Callens, J. Ceulemans, A. Ludwig, P. Foreman, J.P. Remon, Rheological study on mucoadhesivity of some nasal powder formulations, *European Journal of Pharmaceutics and Biopharmaceutics*. 55 (2003) 323–328. [https://doi.org/10.1016/S0939-6411\(03\)00024-9](https://doi.org/10.1016/S0939-6411(03)00024-9).
- [39] G. Colombo, F. Bortolotti, V. Chiapponi, F. Buttini, F. Sonvico, R. Invernizzi, F. Quaglia, C. Danesino, F. Pagella, P. Russo, R. Bettini, P. Colombo, A. Rossi, Nasal powders of thalidomide for local treatment of nose bleeding in persons affected by hereditary hemorrhagic telangiectasia, *International Journal of Pharmaceutics*. 514 (2016) 229–237. <https://doi.org/10.1016/j.ijpharm.2016.07.002>.
- [40] Nasal Spray and Inhalation Solution, Suspension, and spray Drug Products - Chemistry, Manufacturing, and Controls Documentation, (n.d.) 49.
- [41] U.S. Department of Health and Human Services, Food and Drug Administration, Center for Drug Evaluation and Research (CDER), Metered Dose Inhaler (MDI) and Dry Powder Inhaler (DPI) Products - Quality Considerations Guidance for Industry, (2018). <https://www.fda.gov/media/70851/download>.
- [42] European Medicines Agency, GUIDELINE ON THE PHARMACEUTICAL QUALITY OF INHALATION AND NASAL PRODUCTS, (2006). [https://www.ema.europa.eu/en/documents/scientific-guideline/guideline-pharmaceutical-quality-inhalation-nasal-products\\_en.pdf](https://www.ema.europa.eu/en/documents/scientific-guideline/guideline-pharmaceutical-quality-inhalation-nasal-products_en.pdf).
- [43] S. Trows, K. Wuchner, R. Spycher, H. Steckel, Analytical Challenges and Regulatory Requirements for Nasal Drug Products in Europe and the U.S., *Pharmaceutics*. 6 (2014) 195–219. <https://doi.org/10.3390/pharmaceutics6020195>.
- [44] T. Furubayashi, D. Inoue, A. Kamaguchi, Y. Higashi, T. Sakane, Influence of Formulation Viscosity on Drug Absorption Following Nasal Application in Rats, (n.d.) 6.
- [45] S. Horvát, A. Fehér, H. Wolburg, P. Sipos, S. Veszélka, A. Tóth, L. Kis, A. Kurunczi, G. Balogh, L. Kürti, I. Erős, P. Szabó-Révész, M.A. Deli, Sodium hyaluronate as a mucoadhesive component in nasal formulation enhances delivery of molecules to brain tissue, *European Journal of Pharmaceutics and Biopharmaceutics*. 72 (2009) 252–259. <https://doi.org/10.1016/j.ejpb.2008.10.009>.
- [46] T.-W. Chung, D.-Z. Liu, J.-S. Yang, Effects of interpenetration of thermo-sensitive gels by crosslinking of chitosan on nasal delivery of insulin: In vitro characterization and in vivo study, *Carbohydrate Polymers*. 82 (2010) 316–322. <https://doi.org/10.1016/j.carbpol.2010.04.068>.
- [47] C. Hasçıçek, N. Gönül, N. Erk, Mucoadhesive microspheres containing gentamicin sulfate for nasal administration: preparation and in vitro characterization, *Il Farmaco*. 58 (2003) 11–16. [https://doi.org/10.1016/S0014-827X\(02\)00004-6](https://doi.org/10.1016/S0014-827X(02)00004-6).
- [48] K. Pathak, Mucoadhesion; A prerequisite or a constraint in nasal drug delivery?, *International Journal of Pharmaceutical Investigation*. 1 (2011) 62. <https://doi.org/10.4103/2230-973X.82383>.
- [49] U. Anand, T. Feridooni, R. U., Novel Mucoadhesive Polymers for Nasal Drug Delivery, in: A.D. Sezer (Ed.), *Recent Advances in Novel Drug Carrier Systems*, InTech, 2012. <https://doi.org/10.5772/52560>.
- [50] Y.-H. Liao, S.A. Jones, B. Forbes, G.P. Martin, M.B. Brown, Hyaluronan: Pharmaceutical Characterization and Drug Delivery, *Drug Delivery*. 12 (2005) 327–342. <https://doi.org/10.1080/10717540590952555>.
- [51] J. Ding, R. He, G. Zhou, C. Tang, C. Yin, Multilayered mucoadhesive hydrogel films based on thiolated hyaluronic acid and polyvinylalcohol for insulin delivery, *Acta Biomaterialia*. 8 (2012) 3643–3651. <https://doi.org/10.1016/j.actbio.2012.06.027>.
- [52] S.T. Lim, G.P. Martin, D.J. Berry, M.B. Brown, Preparation and evaluation of the in vitro drug release properties and mucoadhesion of novel microspheres of hyaluronic acid and chitosan,

- Journal of Controlled Release. 66 (2000) 281–292. [https://doi.org/10.1016/S0168-3659\(99\)00285-0](https://doi.org/10.1016/S0168-3659(99)00285-0).
- [53] A.K. Bajpai, S.K. Shukla, S. Bhanu, S. Kankane, Responsive polymers in controlled drug delivery, *Progress in Polymer Science*. 33 (2008) 1088–1118. <https://doi.org/10.1016/j.progpolymsci.2008.07.005>.
- [54] R. Zelkó, K. Süvegh, Correlation between the release characteristics of theophylline and the free volume of polyvinylpyrrolidone, *European Journal of Pharmaceutical Sciences*. 24 (2005) 351–354. <https://doi.org/10.1016/j.ejps.2004.11.009>.
- [55] C.P. Tan, N. Anarjan, H.J. Malmiri, I.A. Nehdi, H.M. Sbihi, S.I. Al-Resayes, Effects of homogenization process parameters on physicochemical properties of astaxanthin nanodispersions prepared using a solvent-diffusion technique, *International Journal of Nanomedicine*. (2015) 1109. <https://doi.org/10.2147/IJN.S72835>.
- [56] B. Sinha, R.H. Müller, J.P. Möschwitzer, Bottom-up approaches for preparing drug nanocrystals: Formulations and factors affecting particle size, *International Journal of Pharmaceutics*. 453 (2013) 126–141. <https://doi.org/10.1016/j.ijpharm.2013.01.019>.
- [57] T. Horváth, R. Ambrus, P. Szabóné Révész, Nazális gyógyszerformák permeabilitási vizsgálata Side-Bi-Side™ horizontális cella alkalmazásával, *Acta Pharmaceutica Hungarica*. (2015) 1–10.
- [58] D.M. Vasa, L.A. O'Donnell, P.L.D. Wildfong, Influence of Dosage Form, Formulation, and Delivery Device on Olfactory Deposition and Clearance: Enhancement of Nose-to-CNS Uptake, *Journal of Pharmaceutical Innovation*. 10 (2015) 200–210. <https://doi.org/10.1007/s12247-015-9222-9>.
- [59] H. Jones, Y. Chen, C. Gibson, T. Heimbach, N. Parrott, S. Peters, J. Snoeys, V. Upreti, M. Zheng, S. Hall, Physiologically based pharmacokinetic modeling in drug discovery and development: A pharmaceutical industry perspective, *Clinical Pharmacology & Therapeutics*. 97 (2015) 247–262. <https://doi.org/10.1002/cpt.37>.
- [60] R. Booth, H. Kim, Characterization of a microfluidic in vitro model of the blood-brain barrier ( $\mu$ BBB), *Lab on a Chip*. 12 (2012) 1784. <https://doi.org/10.1039/c2lc40094d>.
- [61] P. Gieszinger, R. Ambrus, C. Bartos, P. Szabóné Révész, Nazális készítmények aktualitásai; bevételre alkalmas eszközök és modern szerelékek, *Gyógyszerészet*. (2017) 204–211.
- [62] S. Naik, B. Chaudhuri, Quantifying Dry Milling in Pharmaceutical Processing: A Review on Experimental and Modeling Approaches, *Journal of Pharmaceutical Sciences*. 104 (2015) 2401–2413. <https://doi.org/10.1002/jps.24512>.
- [63] P.V. Torres-Ortega, L. Saludas, A.S. Hanafy, E. Garbayo, M.J. Blanco-Prieto, Micro- and nanotechnology approaches to improve Parkinson's disease therapy, *Journal of Controlled Release*. 295 (2019) 201–213. <https://doi.org/10.1016/j.jconrel.2018.12.036>.
- [64] J. Kreuter, Nanoparticles—a historical perspective, *International Journal of Pharmaceutics*. 331 (2007) 1–10. <https://doi.org/10.1016/j.ijpharm.2006.10.021>.
- [65] L. Kürti, Á. Kukovecz, G. Kozma, R. Ambrus, M.A. Deli, P. Szabó-Révész, Study of the parameters influencing the co-grinding process for the production of meloxicam nanoparticles, *Powder Technology*. 212 (2011) 210–217. <https://doi.org/10.1016/j.powtec.2011.05.018>.
- [66] G. Sandri, M.C. Bonferoni, S. Rossi, F. Ferrari, S. Gibin, Y. Zambito, G. Di Colo, C. Caramella, Nanoparticles based on N-trimethylchitosan: Evaluation of absorption properties using in vitro (Caco-2 cells) and ex vivo (excised rat jejunum) models, *European Journal of Pharmaceutics and Biopharmaceutics*. 65 (2007) 68–77. <https://doi.org/10.1016/j.ejpb.2006.07.016>.
- [67] F. Sabir, R. Ismail, I. Csoka, Nose-to-brain delivery of anti-glioblastoma drugs embedded into lipid nanocarrier systems: status quo and outlook, *Drug Discovery Today*. (2019). <https://doi.org/10.1016/j.drudis.2019.10.005>.
- [68] A.B. Jindal, The effect of particle shape on cellular interaction and drug delivery applications of micro- and nanoparticles, *International Journal of Pharmaceutics*. 532 (2017) 450–465. <https://doi.org/10.1016/j.ijpharm.2017.09.028>.
- [69] A.S. Macedo, P.M. Castro, L. Roque, N.G. Thomé, C.P. Reis, M.E. Pintado, P. Fonte, Novel and revisited approaches in nanoparticle systems for buccal drug delivery, *Journal of Controlled Release*. 320 (2020) 125–141. <https://doi.org/10.1016/j.jconrel.2020.01.006>.
- [70] K. Ueda, K. Higashi, K. Yamamoto, K. Moribe, In situ molecular elucidation of drug supersaturation achieved by nano-sizing and amorphization of poorly water-soluble drug, *European Journal of Pharmaceutical Sciences*. 77 (2015) 79–89. <https://doi.org/10.1016/j.ejps.2015.05.027>.

- [71] Y. Zhou, Z. Peng, E.S. Seven, R.M. Leblanc, Crossing the blood-brain barrier with nanoparticles, *Journal of Controlled Release*. 270 (2018) 290–303. <https://doi.org/10.1016/j.jconrel.2017.12.015>.
- [72] M. Yasir, U.V.S. Sara, Solid lipid nanoparticles for nose to brain delivery of haloperidol: in vitro drug release and pharmacokinetics evaluation, *Acta Pharmaceutica Sinica B*. 4 (2014) 454–463. <https://doi.org/10.1016/j.apsb.2014.10.005>.
- [73] B.B.S. Cerqueira, A. Lasham, A.N. Shelling, R. Al-Kassas, Nanoparticle therapeutics: Technologies and methods for overcoming cancer, *European Journal of Pharmaceutics and Biopharmaceutics*. 97 (2015) 140–151. <https://doi.org/10.1016/j.ejpb.2015.10.007>.
- [74] H. Chen, C. Khemtong, X. Yang, X. Chang, J. Gao, Nanonization strategies for poorly water-soluble drugs, *Drug Discovery Today*. 16 (2011) 354–360. <https://doi.org/10.1016/j.drudis.2010.02.009>.
- [75] C.M. Keck, R.H. Müller, Nanotoxicological classification system (NCS) – A guide for the risk-benefit assessment of nanoparticulate drug delivery systems, *European Journal of Pharmaceutics and Biopharmaceutics*. 84 (2013) 445–448. <https://doi.org/10.1016/j.ejpb.2013.01.001>.
- [76] R.H. Müller, S. Gohla, C.M. Keck, State of the art of nanocrystals – Special features, production, nanotoxicology aspects and intracellular delivery, *European Journal of Pharmaceutics and Biopharmaceutics*. 78 (2011) 1–9. <https://doi.org/10.1016/j.ejpb.2011.01.007>.
- [77] L. Kürti, R. Gáspár, Á. Márki, E. Kápolna, A. Bocsik, S. Veszélka, C. Bartos, R. Ambrus, M. Vastag, M.A. Deli, P. Szabó-Révész, In vitro and in vivo characterization of meloxicam nanoparticles designed for nasal administration, *European Journal of Pharmaceutical Sciences*. 50 (2013) 86–92. <https://doi.org/10.1016/j.ejps.2013.03.012>.
- [78] R. Ambrus, P. Kocbek, J. Kristl, R. Šibanc, R. Rajkó, P. Szabó-Révész, Investigation of preparation parameters to improve the dissolution of poorly water-soluble meloxicam, *International Journal of Pharmaceutics*. 381 (2009) 153–159. <https://doi.org/10.1016/j.ijpharm.2009.07.009>.
- [79] L. Peltonen, J. Hirvonen, Pharmaceutical nanocrystals by nanomilling: critical process parameters, particle fracturing and stabilization methods: Nanocrystals by nanomilling, *Journal of Pharmacy and Pharmacology*. 62 (2010) 1569–1579. <https://doi.org/10.1111/j.2042-7158.2010.01022.x>.
- [80] R. Abellan-Pose, M. Rodríguez-Évora, S. Vicente, N. Csaba, C. Évora, M.J. Alonso, A. Delgado, Biodistribution of radiolabeled polyglutamic acid and PEG-polyglutamic acid nanocapsules, *European Journal of Pharmaceutics and Biopharmaceutics*. 112 (2017) 155–163. <https://doi.org/10.1016/j.ejpb.2016.11.015>.
- [81] J. Crecente-Campo, S. Lorenzo-Abalde, A. Mora, J. Marzoa, N. Csaba, J. Blanco, Á. González-Fernández, M.J. Alonso, Bilayer polymeric nanocapsules: A formulation approach for a thermostable and adjuvanted E. coli antigen vaccine, *Journal of Controlled Release*. 286 (2018) 20–32. <https://doi.org/10.1016/j.jconrel.2018.07.018>.
- [82] P. Gieszinger, I. Csóka, E. Pallagi, G. Katona, O. Jójárt-Laczkovich, P. Szabó-Révész, R. Ambrus, Preliminary study of nanonized lamotrigine containing products for nasal powder formulation, *Drug Design, Development and Therapy*. Volume 11 (2017) 2453–2466. <https://doi.org/10.2147/DDDT.S138559>.
- [83] P. Gieszinger, I. Tomuta, T. Casian, Cs. Bartos, P. Szabó-Révész, R. Ambrus, Definition and validation of the Design Space for co-milled nasal powder containing nanosized lamotrigine, *Drug Development and Industrial Pharmacy*. 44 (2018) 1622–1630. <https://doi.org/10.1080/03639045.2018.1483388>.
- [84] J.V. González-Aramundiz, E. Presas, I. Dalmau-Mena, S. Martínez-Pulgarín, C. Alonso, J.M. Escribano, M.J. Alonso, N.S. Csaba, Rational design of protamine nanocapsules as antigen delivery carriers, *Journal of Controlled Release*. 245 (2017) 62–69. <https://doi.org/10.1016/j.jconrel.2016.11.012>.
- [85] L.N. Thwala, D.P. Delgado, K. Leone, I. Marigo, F. Benetti, M. Chenlo, C.V. Alvarez, S. Tovar, C. Dieguez, N.S. Csaba, M.J. Alonso, Protamine nanocapsules as carriers for oral peptide delivery, *Journal of Controlled Release*. 291 (2018) 157–168. <https://doi.org/10.1016/j.jconrel.2018.10.022>.
- [86] I. Santalices, D. Torres, M.V. Lozano, M.M. Arroyo-Jiménez, M.J. Alonso, M.J. Santander-Ortega, Influence of the surface properties of nanocapsules on their interaction with intestinal barriers, *European Journal of Pharmaceutics and Biopharmaceutics*. 133 (2018) 203–213. <https://doi.org/10.1016/j.ejpb.2018.09.023>.

- [87] P. Agrawal, R.P. Singh, Sonali, L. Kumari, G. Sharma, B. Koch, C.V. Rajesh, A.K. Mehata, S. Singh, B.L. Pandey, M.S. Muthu, TPGS-chitosan cross-linked targeted nanoparticles for effective brain cancer therapy, *Materials Science and Engineering: C*. 74 (2017) 167–176. <https://doi.org/10.1016/j.msec.2017.02.008>.
- [88] P. Jakubiak, L.N. Thwala, A. Cadete, V. Pr eat, M.J. Alonso, A. Beloqui, N. Csaba, Solvent-free protamine nanocapsules as carriers for mucosal delivery of therapeutics, *European Polymer Journal*. 93 (2017) 695–705. <https://doi.org/10.1016/j.eurpolymj.2017.03.049>.
- [89] S. El-Safy, S.N. Tammam, M. Abdel-Halim, M.E. Ali, J. Youshia, M.A. Shetab Boushehri, A. Lamprecht, S. Mansour, Collagenase loaded chitosan nanoparticles for digestion of the collagenous scar in liver fibrosis: The effect of chitosan intrinsic collagen binding on the success of targeting, *European Journal of Pharmaceutics and Biopharmaceutics*. 148 (2020) 54–66. <https://doi.org/10.1016/j.ejpb.2020.01.003>.
- [90] E. Muntimadugu, R. Dhommati, A. Jain, V.G.S. Challa, M. Shaheen, W. Khan, Intranasal delivery of nanoparticle encapsulated tarenflurbil: A potential brain targeting strategy for Alzheimer’s disease, *European Journal of Pharmaceutical Sciences*. 92 (2016) 224–234. <https://doi.org/10.1016/j.ejps.2016.05.012>.
- [91] Y.S.R. Elnaggar, S.M. Etman, D.A. Abdelmonsif, O.Y. Abdallah, Intranasal Piperine-Loaded Chitosan Nanoparticles as Brain-Targeted Therapy in Alzheimer’s Disease: Optimization, Biological Efficacy, and Potential Toxicity, *Journal of Pharmaceutical Sciences*. 104 (2015) 3544–3556. <https://doi.org/10.1002/jps.24557>.
- [92] S.S. Chudiwal, M.H.G. Dehghan, Quality by design approach for development of suspension nasal spray products: a case study on budesonide nasal suspension, *Drug Development and Industrial Pharmacy*. 42 (2016) 1643–1652. <https://doi.org/10.3109/03639045.2016.1160108>.
- [93] E. Pallagi, K. Karimi, R. Ambrus, P. Szab o-R ev esz, I. Cs oka, New aspects of developing a dry powder inhalation formulation applying the quality-by-design approach, *International Journal of Pharmaceutics*. 511 (2016) 151–160. <https://doi.org/10.1016/j.ijpharm.2016.07.003>.
- [94] B.S. Riley, X. Li, Quality by Design and Process Analytical Technology for Sterile Products—Where Are We Now?, *AAPS PharmSciTech*. 12 (2011) 114–118. <https://doi.org/10.1208/s12249-010-9566-x>.
- [95] A. Solaiman, A.S. Suliman, S. Shinde, S. Naz, A.A. Elkordy, Application of general multilevel factorial design with formulation of fast disintegrating tablets containing croscaremellose sodium and Disintequick MCC-25, *International Journal of Pharmaceutics*. 501 (2016) 87–95. <https://doi.org/10.1016/j.ijpharm.2016.01.065>.
- [96] A. Porfire, D.M. Muntean, L. Rus, B. Sylvester, I. Tomu a, A quality by design approach for the development of lyophilized liposomes with simvastatin, *Saudi Pharmaceutical Journal*. 25 (2017) 981–992. <https://doi.org/10.1016/j.jsps.2017.01.007>.
- [97] D. Hales, L. Vlase, S.A. Porav, A. Bodoki, L. Barbu-Tudoran, M. Achim, I. Tomu a, A quality by design (QbD) study on enoxaparin sodium loaded polymeric microspheres for colon-specific delivery, *European Journal of Pharmaceutical Sciences*. 100 (2017) 249–261. <https://doi.org/10.1016/j.ejps.2017.01.006>.
- [98] S. Iurian, L. Turdean, I. Tomuta, Risk assessment and experimental design in the development of a prolonged release drug delivery system with paliperidone, *Drug Design, Development and Therapy*. Volume11 (2017) 733–746. <https://doi.org/10.2147/DDDT.S125323>.
- [99] T. Casian, S. Iurian, C. Bogdan, L. Rus, M. Moldovan, I. Tomuta, QbD for pediatric oral lyophilisates development: risk assessment followed by screening and optimization, *Drug Development and Industrial Pharmacy*. 43 (2017) 1932–1944. <https://doi.org/10.1080/03639045.2017.1350702>.
- [100] S. Iurian, I. Tomuta, C. Bogdan, L. Rus, T. Tokes, L. Barbu-Tudoran, M. Achim, M. Moldovan, S. Leucuta, Defining the design space for freeze-dried orodispersible tablets with meloxicam, *Drug Development and Industrial Pharmacy*. 42 (2016) 1977–1989. <https://doi.org/10.1080/03639045.2016.1188108>.
- [101] S. Soltanpour, A. Jouyban, Solubility of lamotrigine in binary and ternary mixtures of N-methyl pyrrolidone and water with polyethylene glycols 200, 400, and 600 at 298.2K, *Journal of Molecular Liquids*. 180 (2013) 1–6. <https://doi.org/10.1016/j.molliq.2012.12.029>.
- [102] K. Mohana Raghava Srivalli, P.K. Lakshmi, J. Balasubramaniam, Design of a novel bilayered gastric mucoadhesive system for localized and unidirectional release of lamotrigine, *Saudi Pharmaceutical Journal*. 21 (2013) 45–52. <https://doi.org/10.1016/j.jsps.2012.01.004>.
- [103] S. Gizurason, Anatomical and Histological Factors Affecting Intranasal Drug and Vaccine Delivery, *CDD*. 9 (2012) 566–582. <https://doi.org/10.2174/156720112803529828>.

- [104] S. Gizurarson, The relevance of nasal physiology to the design of drug absorption studies, *Advanced Drug Delivery Reviews*. 11 (1993) 329–347. [https://doi.org/10.1016/0169-409X\(93\)90015-V](https://doi.org/10.1016/0169-409X(93)90015-V).
- [105] L. Kozlovskaya, M. Abou-Kaoud, D. Stepensky, Quantitative analysis of drug delivery to the brain via nasal route, *Journal of Controlled Release*. 189 (2014) 133–140. <https://doi.org/10.1016/j.jconrel.2014.06.053>.
- [106] Y. Zhang, M. Huo, J. Zhou, S. Xie, PKSolver: An add-in program for pharmacokinetic and pharmacodynamic data analysis in Microsoft Excel, *Computer Methods and Programs in Biomedicine*. 99 (2010) 306–314. <https://doi.org/10.1016/j.cmpb.2010.01.007>.
- [107] Guidance for Industry Considering Whether an FDA-Regulated Product Involves the Application of Nanotechnology, *Biotechnology Law Report*. 30 (2011) 613–616. <https://doi.org/10.1089/blr.2011.9814>.
- [108] L.M. Ensign, C. Schneider, J.S. Suk, R. Cone, J. Hanes, Mucus Penetrating Nanoparticles: Biophysical Tool and Method of Drug and Gene Delivery, *Advanced Materials*. 24 (2012) 3887–3894. <https://doi.org/10.1002/adma.201201800>.



## ACKNOWLEDGMENTS

I would like to express my sincere gratitude to the Head of the Institute of Pharmaceutical Technology and Regulatory Affairs **Dr. habil. Ildikó Csóka** for providing me with the opportunity to work in this department and complete my Ph.D. work under their expert guidance. I am grateful to my supervisors **Dr. Rita Ambrus Ph.D.** and **Prof. Dr. Piroska Szabó-Révész DSc** for their scientific guidance, encouragement, and support throughout my Ph.D. studies.

I am thankful to my co-authors and cooperation partners for their inspiring help in my studies during train ships:

**Dr. Gábor Katona, Dr. Orsolya Jójárt-Laczkovich, Dr. Edina Pallagi, Dr. Csilla Bartos** and **Tamas Kiss**, Institute of Pharmaceutical Technology and Regulatory Affairs, University of Szeged

**Prof. Ioan Tomuta, Dr. Tibor. Casian**, Department of Pharmaceutical Technology and Biopharmacy, Iuliu Hatieganu University of Medicine and Pharmacy,

**Dr. Noemi Stefania Csaba, Dr. Marcos Garcia-Fuentes, Maruthi Prasanna Ph.D.**, Center for Research in Molecular Medicine and Chronic Diseases (CiMUS), University of Santiago de Compostela.

I would like to thank **Erika Boda Feczko** and **Piroska Lakatos** for excellent technical assistance. I would like to thank all members of the Institute of Pharmaceutical Technology and Regulatory Affairs for their help and friendship.

I would like to thanks to the financial and cooperation support to the:

This work was supported by *the Ministry of Human Capacities, Hungary grant* (20391-3/2018/FEKUSTRAT).

This work was supported by the *New National Excellence Program of the Ministry of Human Capacities* (UNKP-19-3-SZTE-53).

This work was supported by the GINOP-2.3.2-15-2016-00060- Development and targeting new active pharmaceutical ingredients by means of new drug-carrier systems- project.

This work was supported by the *National Research Development and Innovation Office* and *Richter Plc., Budapest, Hungary* (GINOP 2.2.1-15-2016-00007).

The *Central European Exchange Programme for University Studies (CEEPUS)* for my short study support at University of Graz.

*Exchange Agreement between* Center for Research in Molecular Medicine and Chronic Diseases (CiMUS), University of Santiago de Compostela and the University of Szeged, Faculty of Pharmacy.

*Tempus Public Foundation and Campus Mundi Student Mobility* for short study support at Center for Research in Molecular Medicine and Chronic Diseases (CiMUS), University of Santiago de Compostela.

Finally, I am especially thankful to my **family** and **friends** for their love and unstinting support during my studies.